สารยับยั้งแอลฟากลูโคซิเดสจากหญ้าหนวดแมว *Orthosiphon aristatus* Miq

นางสาวดวงกมล ท่วมสุข



วิทยานิพนธ์นี้เป็นส่วนหนึ่งของการศึกษาตามหลักสูตรปริญญาวิทยาศาสตรมหาบัณฑิต
สาขาวิชาเทคโนโลยีชีวภาพ
คณะวิทยาศาสตร์ จุฬาลงกรณ์มหาวิทยาลัย
ปีการศึกษา 2557

# α-GLUCOSIDASE INHIBITORS FROM JAVA TEA *Orthosiphon aristatus* Miq

Miss Doungkamon Toumsuk


A Thesis Submitted in Partial Fulfillment of the Requirements

for the Degree of Master of Science Program in Biotechnology

Faculty of Science

Chulalongkorn University

Academic Year 2014

| | |
|---|---|
| Thesis Title | α-GLUCOSIDASE INHIBITORS FROM JAVA TEA *Orthosiphon aristatus* Miq |
| By | Miss Doungkamon Toumsuk |
| Field of Study | Biotechnology |
| Thesis Advisor | Assistant Professor Preecha Phuwapraisirisan, Ph.D. |

Accepted by the Faculty of Science, Chulalongkorn University in Partial Fulfillment of the Requirements for the Master's Degree

.....Dean of the Faculty of Science
(Professor Supot Hannongbua, Dr.rer.nat.)

THESIS COMMITTEE

.....Chairman
(Associate Professor Vudhichai Parasuk, Ph.D.)

.....Thesis Advisor
(Assistant Professor Preecha Phuwapraisirisan, Ph.D.)

.....Examiner
(Assistant Professor Kanoktip Packdibamrung, Ph.D.)

.....External Examiner
(Assistant Professor Wimolpun Rungprom, Ph.D.)

ดวงกมล ท่วมสุข : สารยับยั้งแอลฟากลูโคซิเดสจากหญ้าหนวดแมว *Orthosiphon aristatus* Miq (α-GLUCOSIDASE INHIBITORS FROM JAVA TEA *Orthosiphon aristatus* Miq) อ.ที่ปรึกษาวิทยานิพนธ์หลัก: ปรีชา ภูวไพรศิริศาล, 48 หน้า.

โรคเบาหวานเป็นโรคที่เกิดจากการทำงานที่ผิดปกติของระบบการดูดซึมกลูโคสในกระแสเลือด โรคเบาหวานชนิดที่ 2 เกิดจากการที่ร่ายกายไม่ตอบสนองต่ออินซูลินหรือการหลั่งอินซูลินที่ลดลง การรักษาเบาหวานชนิดที่ 2 อย่างมีประสิทธิภาพจำเป็นที่จะต้องลดระดับกลูโคสโดยการยับยั้งการทำงานของเอมไซม์แอลฟากลูโคสซิเดสจากลำไส้เล็ก Java tea *Orthosiphon aristatus* (Blume) Miq. หรือชื่อในภาษาไทยเรียกว่าหญ้าหนวดแมว เนื่องจากมีรายงานว่าสามารถยับยั้งภาวะน้ำตาลในเลือดสูงในสัตว์ทดลอง ในงานวิจัยนี้เราได้เตรียมสารสกัดจากใบและกิ่งของหญ้าหนวดแมว โดยใช้วิธีที่แตกต่างกัน 2 วิธี คือ การสกัดแบบยาต้มและการสกัดแบบหมักแช่ เพื่อทำการคัดเลือกหาประสิทธิภาพการยับยั้งแอลฟากลูโคสซิเดสที่ดีที่สุด ผลการทดลองได้ชี้ชัดว่าสารสกัดจากใบที่เตรียมโดยการต้มด้วยน้ำร้อนสามารถยับยั้งการทำงานของเอนไซม์ได้อย่างมีศักยภาพมากขึ้น การแยกสารสกัดน้ำจากของใบโดยผลการทดสอบฤทธิ์ทางชีวภาพชี้นำสามารถแยกสารได้ 4 ชนิด คือ methyl caffeate (1), 3,4-dihydroxy benzaldehyde (2), methyl rosmarinate (3) และ rosmarinic acid (4) ซึ่งสารที่แยกได้เหล่านี้สามารถยังยั้งเอนไซม์ maltase และ sucrase ที่ค่า $IC_{50}$ ในช่วงระหว่าง 0.061-0.738 mM ซึ่งมีประสิทธิภาพมากกว่าacarbose ซึ่งใช้เป็นสารมาตรฐานในการเปรียบเทียบ นอกจากนี้การศึกษาจลนพลศาสตร์ของสารยังพบว่า methyl rosmarinate และ rosmarinic acid สามารถยับยั้งเอนไซม์ maltase แบบ mixed-type ขณะที่เอนไซม์ sucrase ถูกยับยั้งแบบ mixed-type และแบบ competitive



สาขาวิชา เทคโนโลยีชีวภาพ ลายมือชื่อนิสิต .....

ปีการศึกษา 2557 ลายมือชื่อ อ.ที่ปรึกษาหลัก .....

# # 5572246823 : MAJOR BIOTECHNOLOGY
KEYWORDS: DIABETES / ORTHOSIPHON ARISTATUS / ALPHA-GLUCOSIDASE INHIBITOR

DOUNGKAMON TOUMSUK: α-GLUCOSIDASE INHIBITORS FROM JAVA TEA *Orthosiphon aristatus* Miq. ADVISOR: ASST. PROF. PREECHA PHUWAPRAISIRISAN, Ph.D., 48 pp.

Diabetes is a metabolic disorder where the body fails to utilize the ingested glucose properly. Type 2 diabetes is characterized by insulin resistance, which may be combined with relatively reduced insulin secretion. An effective strategy for type 2 diabetes therapy is to suppress glucose level through inhibition of intestinal α-glucosidase. *Orthosiphon aristatus* (Blume) Miq. (Java tea) known in Thai as "Ya-Nuad-Meo" have been recorded for in *vivo* hyperglycemia. In our research, crude extracts from leaves and twigs of *O. aristatus* prepared by two different extraction methods-decoction and maceration were screened for a-glucosidase inhibition. Apparently, the leave extract prepared by decoction with hot water showed more potent inhibition. Bioassay-guided fractionation of the aqueous extract from leaves led to the isolation of methyl caffeate (1), 3,4-dihydroxy benzaldehyde (2), methyl rosmarinate (3) and rosmarinic acid (4). The isolated compounds inhibited maltase and sucrase with $IC_{50}$ values in the range of 0.061-0.738 mM, which are equipotent to standard antidiabetic drug acarbose. Furthermore, the kinetic investigation revealed that maltase was inhibited by methyl rosmarinate and rosmarinic acid through mixed-type whereas sucrase was inhibited through mixed-type and competitive manners.



Field of Study: Biotechnology Student's Signature .....

Academic Year: 2014 Advisor's Signature .....

## ACKNOWLEDGEMENTS

I would like to express my deepest appreciation to my advisor, Assistant Professor Dr. Preecha Phuwapraisirisan for encouragement and support at all time of this research.

I would like to gratefully acknowledge the members of the thesis committees, Associate Professor Dr. Vudhichai Parasuk, Assistant Professor Dr. Kanoktip Packdibamrung and Assistant Professor Dr.Wimolpun Rungpromfor discussion, guidance and extending cooperation over my presentation.

I would like to express my gratitude to Natural Products Research Unit, Department of Chemistry, Faculty of Science, Chulalongkorn University for supporting of chemicals and laboratory facilities throughout the course of study and Program of Biotechnology, Faculty of Science, Chulalongkorn University for giving me a chance to study here.

Finally, I would also like to express my family Dr. Kiettipum Phontree, Dr. Wisuttaya Worawalai, Dr. Thanakorn Damsud and also to my family. Furthermore, all of my friends in the laboratory for their friendships and help during the course of my graduate research.

**CONTENTS**

Page

THAI ABSTRACT ..... iv

ACKNOWLEDGEMENTS ..... vi

CONTENTS ..... vii

LIST OF TABLES ..... ix

LIST OF FIGURES ..... x

LIST OF SCHEMES ..... xii

LIST OF ABBREVIATIONS ..... xiii

CHAPTER I INTRODUCTION ..... 1

1.1 Diabetes and therapy: α-glucosidase inhibition approach ..... 1

1.1.1 Diabetes mellitus (DM) ..... 2

1.1.2 Type 1 and type 2 diabetes ..... 3

1.1.3 Oral anti-hyperglycemic therapy for type 2 diabetes mellitus (α-glucosidase inhibitors) ..... 4

1.2 Plant a source of α-glucosidase inhibitors ..... 8

1.3 *Orthosiphon aristarus* (Blume) Miq.: botanical aspects and literature reviews . 11

CHAPTER II BIOASSAY-GUIDED ISOLATION AND CHARACTER ISOLATION OF α-GLUCOSIDASE INHIBITORS ..... 14

2.1 Preliminary study on extraction method and plant part ..... 14

2.2 Isolation and purification of active components ..... 17

2.3 Identification of Isolation components ..... 19

2.3.1 Structure elucidation of methyl caffeate (1) ..... 19

2.3.2 Structure elucidation of 3,4-dihydroxybenzaldehyde (2) ..... 19

Page

2.3.3 Structure elucidation of methyl rosmarinate (3) ..... 20
2.3.4 Structure elucidation of rosmarinic acid (4) ..... 21
2.4 Inhibitory activity of compounds 1-4 against α-glucosidases ..... 22
2.5 Experimental section ..... 23
2.5.1 General experiment procedures ..... 23
2.5.2 Plant material ..... 23
2.5.3 Extraction and isolation ..... 23
2.5.4 α-Glucosidase inhibitory activity ..... 25
2.5.4.1 Chemical and equipment ..... 25
2.5.4.2 α-Glucosidase inhibitory activity from rat intestinal ..... 25
CHAPTER III KINETIC MECHANISM OF INHIBITORY ..... 28
3.1 Evaluation of kinetic mechanism ..... 28
3.1.1. Kinetic mechanism underlying the inhibition of methyl rosmarinate (3) against rat intestinal glucosidases ..... 28
3.1.2. Kinetic mechanism underlying the inhibition of rosmarinic acid (4) against rat intestinal glucosidases ..... 32
3.2 Experimental section ..... 35
3.2.1 Measurement of kinetic constant ..... 35
CHAPTER IV CONCLUSION ..... 36
REFERENCES ..... 38
VITA ..... 48

# LIST OF TABLES

Table Page

**1.1** α-Glucosidase inhibitors in the clinical practice against T2DM ..... 7

**2.1** α-Glucosidase inhibitory activity of isolated compounds ..... 22

**3.1** Inhibition mechanism ..... 28

**3.2** Kinetic parameters of methyl rosmarinate (**3**) ..... 29

**3.3** Kinetic parameters of rosmarinic acid (**4**) ..... 32

# LIST OF FIGURES

Figure Page

**1.1** Worldwide prevalence of diabetes in 2000 and estimates for the year 2030 (in millions) (http://www.myhealthywaist.org.)..... 1

**1.2** Insulin signaling in peripheral cells. (www.redcrosshr.eu)..... 2

**1.3** Causes of diabetes: insufficient insulin for type 1 DM and insulin resistant for type 2 DM (www.dtc.ucsf.edu/types-of-diabetes). ..... 3

**1.4** Mechanistic inhibition of acarbose against by α-glucosidase located in the intestinal brush border [11]. ..... 5

**1.5** Hydrolysis of oligosaccharides by α-glucosidase..... 6

**1.6** Structures of 1-deoxynojirimycin) DNJ(, miglitol and voglibose..... 9

**1.7** Structures of salacinol and kotalanol ..... 10

**1.8** *Orthosiphon aristatus* (Blume) Miq..... 11

**1.9** Structures of all compounds reported by Di and coworkers. ..... 13

**2.1** α-Glucosidase inhibitory activity of leaves extracts against sucrase (A) and maltase (B) at concentrations of 0.1-10 mg/mL..... 16

**2.2** α-Glucosidase inhibitory activity of twigs extracts against sucrase )A( and maltase (B (at concentrations of 0.1-10 mg/mL..... 16

**3.1** Lineweaver-Burk plot for inhibitory activity of methyl rosmarinate (**3**) against intestinal sucrase..... 30

**3.2** Secondary plot of slope vs. [I] from a Lineweaver-Burk plot for the determination of $K_i$..... 30

**3.3** Secondary plot of intercept vs. [I] from a Lineweaver-Burk plot for the determination of $K_i'$..... 30

**3.4** Lineweaver-Burk plot for inhibitory activity of methyl rosmarinate (**3**) against intestinal maltase..... 31

**3.5** Secondary plot of slope vs. [I] from a Lineweaver-Burk plot for the determination of $K_i$..... 31

**3.6** Secondary plot of intercept vs. [I] from a Lineweaver-Burk plot for the determination of $K_i'$..... 31

**3.7** Lineweaver-Burk plot for inhibitory activity of rosmarinicacid (**4**) against intestinal sucrase. ..... 33

**3.8** Secondary plot of slope *vs*. [I] from a Lineweaver-Burk plot for the determination of $K_i$..... 33

**3.9** Lineweaver-Burk plot for inhibitory activity of rosmarinic acid (**4**) against intestinal maltase. ..... 34

**3.10** Secondary plot of slope *vs*. [I] from a Lineweaver-Burk plot for the determination of $K_i$..... 34

**3.11** Secondary plot of intercept *vs*. [I] from a Lineweaver-Burk plot for the determination of $K_i'$..... 34

**4.1** The chemical structures of isolated compounds from *O. aristatus* leaves **1**-**4** ..... 37

# LIST OF SCHEMES

Scheme Page

**2.1** Extraction methods applied in bioassay screening. ..... 14

**2.2** Isolation procedure ..... 18

**2.3** Hydrolysis of maltose and sucrose by rat intestinal α-glucosidases. ..... 26

# LIST OF ABBREVIATIONS

| | |
|---|---|
| $^{o}C$ | Degree Celsius |
| $CD_3OD$ | Deuterated methanol |
| DMSO | Dimethyl sulfoxide |
| $^{13}C$ NMR | Carbon-13 nuclear magnetic resonance |
| DM | Diabetes mellitus |
| d | Doublet (NMR) |
| dd | Doublet of doublet (NMR) |
| EC | Enzyme Commission |
| ESIMS | Electrospray ionization mass spectrometry |
| Hz | Hertz |
| $IC_{50}$ | Concentration that required for 50% inhibition in *vitro* |
| *J* | Coupling constant |
| kg | Kilogram |
| $K_m$ | Michaelis constant |
| l | Liter |
| μl | Microliter |

| | |
|---|---|
| M | Mole per liter (molar) |
| MW | Molecular weight |
| μM | Micromolar |
| mg | Milligram |
| min | Minute |
| ml | Milliliter |
| mM | Millimolar |
| *m/z* | Mass per charge |
| NMR | Nuclear magnetic resonance |
| nm | Nanometer |
| OD | Optical density |
| s | Singlet (NMR) |
| TLC | Thin-layer chromatography |
| NaCl | Sodium chloride |
| UV | Ultraviolet |
| $V_{max}$ | Maximum velocity |
| δ | Chemical shift |

# CHAPTER I

# INTRODUCTION

## 1.1 Diabetes and therapy: α-glucosidase inhibition approach

Diabetes mellitus is a chronic metabolic disorder characterized by abnormalities in carbohydrate. Currently, 171 million people worldwide are considered to be diabetic and this number is expected to rise to 366 million in year 2030 (Figure 1.1) [1]. This striking prevalence can even be an underestimate due to methodological uncertainties as well as undiagnosed cases [2]. The highest increases are expected in the developing countries of Africa, Asia, and South America, while European populations seem to be less affected [3].

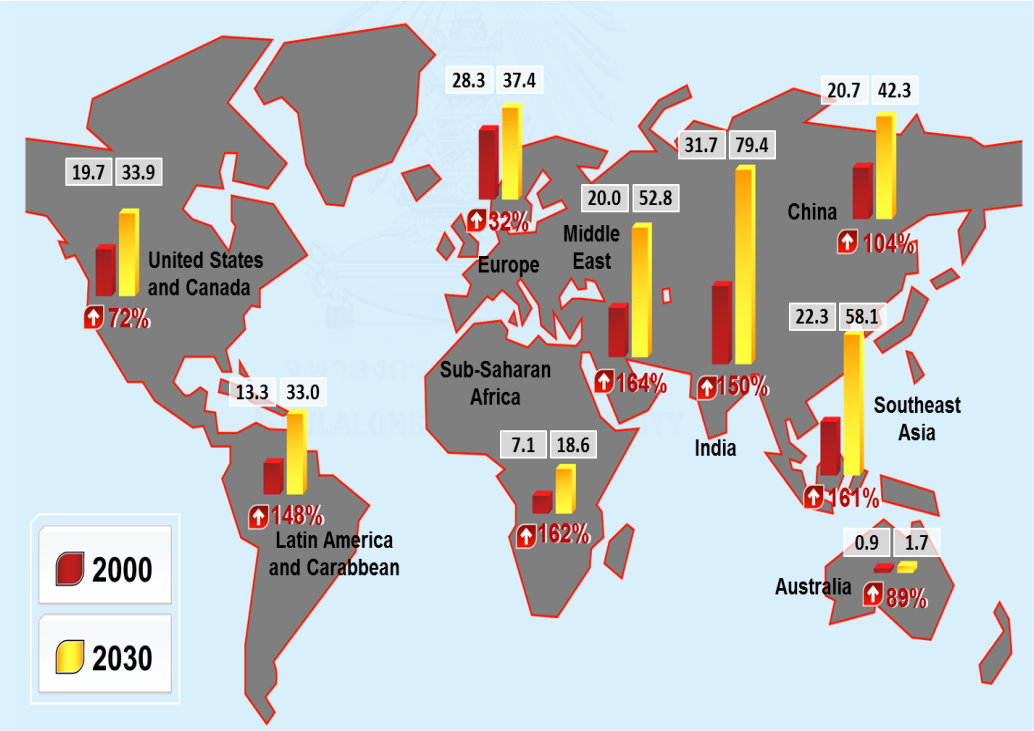


**Figure 1.1** Worldwide prevalence of diabetes in 2000 and estimates for the year 2030 (in millions) (http://www.myhealthywaist.org.)

### 1.1.1 Diabetes mellitus (DM)

Diabetes mellitus is a syndrome consisting of metabolic, vascular, and neuropathic components that are interrelated. It actually is a group of metabolic diseases characterized by hyperglycemia arising as a consequence of a relative or absolute deficiency of insulin secretion, resistance to insulin action, or both [4]

Insulin is a hormone produced by the pancreas. It is secreted directly into the bloodstream to regulate the sugar (glucose) levels in the body. When the person eats or drinks, food is digested into glucose, which is absorbed into the bloodstream and stimulates the pancreas to produce insulin. Thus, glucose is transported into the cells when insulin binds to insulin receptor, which straddles the cell membrane of many cells (Figure 1.2) [5].

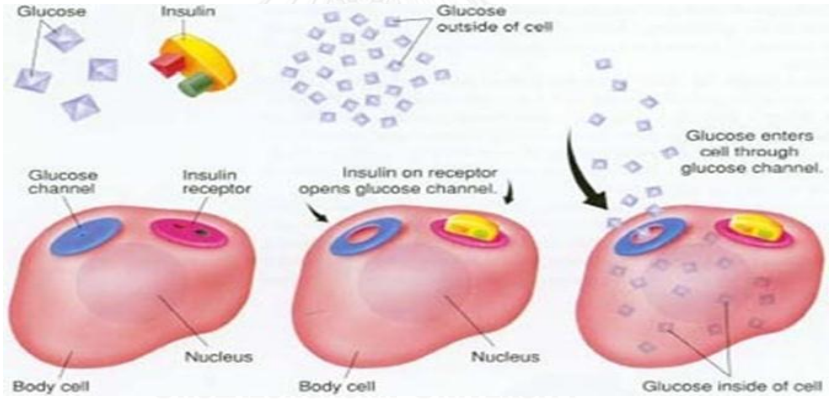


**Figure 1.2** Insulin signaling in peripheral cells. (www.redcrosshr.eu)

The lack of effective insulin action results in alterations of carbohydrate, fat, and protein metabolism. As the chronic hyperglycemia of diabetes, diabetic patients may suffer from the tragic ravages of long-term damage, dysfunction, and failure of various organs, especially eyes, kidneys, nerves, heart, and blood vessels. Although several pathogenic processes may be involved in the development of diabetes, the vast majority of cases are classified into two main categories: type 1 and type 2 diabetes, as illustrated in Figure 1.3 [6].

### 1.1.2 Type 1 and type 2 diabetes

Type 1 DM is characterized by the loss of insulin-secreting capacity due to selective autoimmune destruction of the pancreatic β-cells, leading to a deficiency of insulin (Figure 1.3). Without the presence of insulin, many of the body's cells cannot take glucose from the blood and therefore the body uses other sources of energy. Type 1 DM comprises approximately 5% to 10% of all people with DM. People with type 1 DM require insulin injection to compensate for their body's lack of insulin [7].

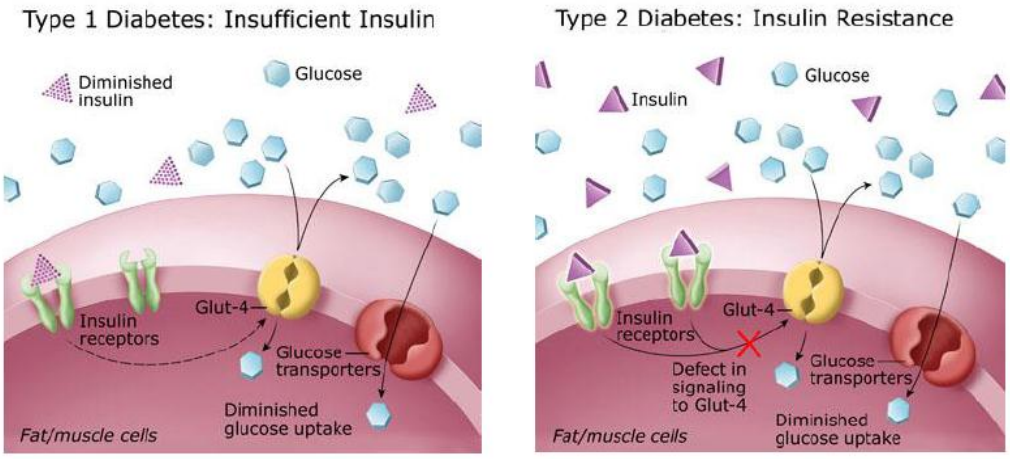


**Figure 1.3** Causes of diabetes: insufficient insulin for type 1 DM and insulin resistant for type 2 DM (www.dtc.ucsf.edu/types-of-diabetes).

Type 2 DM, the more common type, is characterized by a relative insulin deficiency and is associated with insulin resistance in the peripheral tissues (Figure 1.3). As a result, the body is less able to take up glucose from the blood, causing hyperglycemia as well as vascular, nerve and renal complications. This type of DM comprises approximately 90% to 95% of all diabetes patients. It usually occurs in adult, in addition to teenagers. In all probability, the causes of type 2 DM lie in environmental and lifestyle factors. Prominence among these factors is obesity, and approximately 50% to 90% of all patients with type 2 DM are obese [8]. Recently, the prevalence of type 2 DM throughout the world is increasing at an alarming rate.

There are over 173 million people worldwide with type 2 DM. The main complications of type 2 DM are associated with the cardiovascular disease those result in excess morbidity and mortality [1, 9].

There are several approaches for treatment of type 2 DM. Each approach works in different ways to lower blood glucose levels. In the early stages, many people with type 2 DM can control their blood glucose levels by diet, exercise, and weight loss. Most importantly, an efficient therapeutic approach for treatment of type 2 DM is to delay the postprandial hyperglycemia by retarding the rate of carbohydrate digestion through the inhibition of α-glucosidase [10].

### 1.1.3 Oral anti-hyperglycemic therapy for type 2 diabetes mellitus (α-glucosidase inhibitors)

Diabetes treatment mainly depends on the type and severity of the diabetes. Type I diabetes is treated with insulin, exercise, and a diabetic diet. Type II diabetes is first treated with weight reduction, a diabetic diet and exercise. When these treatments fail to control the elevated blood sugars, oral medications are used. If oral medications are still insulin medications, other injectable medications are considered. Oral medications are dividing into three groups, namely insulin secreatagogue, insulin sensitizer and α-glucosidase inhibitors [11].

A potential therapeutic approach is to suppress the postprandial hyperglycemia by retarding absorption of glucose through inhibition of carbohydrate-hydrolyzing enzymes, collectively named α-glucosidase (sucrase, maltase and isomaltase) in the digestive trace of the small intestine (Figure 1.4).

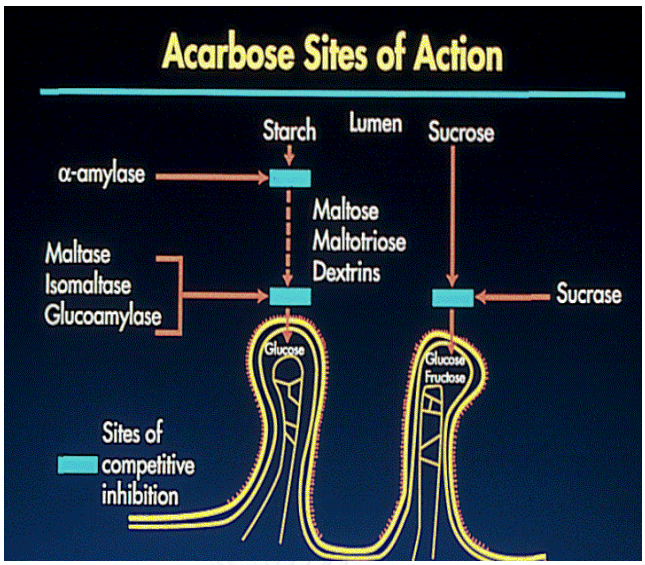


**Figure 1.4** Mechanistic inhibition of acarbose against by α-glucosidase located in the intestinal brush border [11].

α-Glucosidase catalyzes the hydrolysis of α-glucosidic bond from the non-reducing end of a chain, together with α-glucosidic bond of free disaccharides. The enzyme, which belongs to glycoside hydrolases family 13, has common specific structural features such as the catalytic $(\beta/\alpha)_8$-barrel domain, which acts specifically on α-1,4-O-glucosidic linkages (Figure 1.5) [12]. Inhibitors of these enzyme delay carbohydrate digestion and prolong overall carbohydrate digestion time, causing a decline in the rate of glucose absorption and consequently suppressing the postprandial plasma glucose level [13].

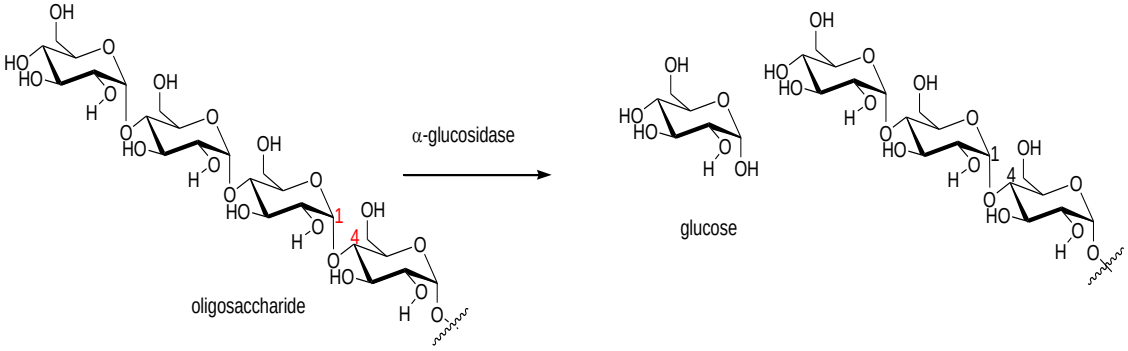


**Figure 1.5** Hydrolysis of oligosaccharides by α-glucosidase.

To date, prominent α-glucosidases inhibitors such as acarbose, miglitol, and voglibose [14] (Table1.1) are used as drugs in the treatment of T2DM under various brand names. These compounds are known to inhibit a wide range of glucosidases. In the absence of specificity and because of the known serious side effects, the applications of these first generation iminosugar drugs are limited. Current investigations aim at discovering safer, more specific, and effective iminosugar based derivatives not only as hypoglycemic agents but also as other specific therapy [15].

**Table 1.1** α-Glucosidase inhibitors in the clinical practice against T2DM

| Name | Structure | Side-effect |
|---|---|---|
| Acarbose | 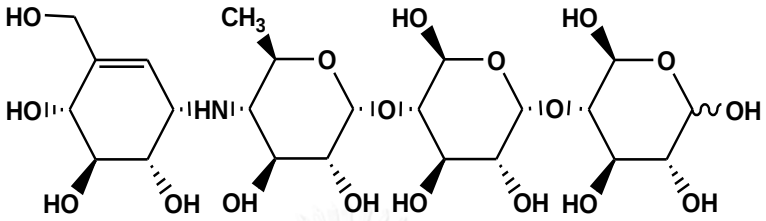 | Flatulence (78% of the patients) Diarrhea (14% of the patients) |
| Miglitol | 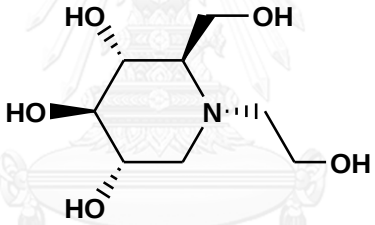 | Diarrhea, gas, soft stools, stomach pain |
| Voglibose | 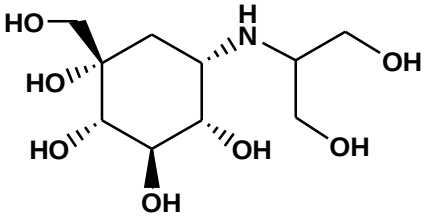 | Diarrhea, stool loss, meteorism, upset stomach |

### 1.2 Plant a source of α-glucosidase inhibitors

Current scientific evidence demonstrates that much of the morbidity and mortality of diabetes can be eliminated by aggressive treatment with diet, exercise, and new pharmacological approaches to achieve better control of blood glucose level. Furthermore, the possibility of preventing the onset of diabetes using dietary supplements and herbal medicines has attracted increasing attention. Herbal medicines are prescribed widely because of their effectiveness, fewer side effect and relatively low cost. To this end, research has begun to embrace traditional medicines from various cultures, as scientists search for clues to discover new therapeutic drugs for diabetes [16]. Traditional Indian and Chinese medicine have long used plant and herbal extracts as anti-diabetic agents [17]. Therefore, investigation on such agents from traditional medicinal plants has become more important and researches are competing to find the new effective and safe therapeutic agents for the treatment of diabetes.

A prominent example of natural α-glucosidase inhibitor includes 1-deoxynojirimycin (DNJ, Figure 1.6) which was first isolated from the roots of mulberry [18]. DNJ is also produced by many strains of *Bacillus* and *Streptomyces*, which shows potent inhibition against both α- and β-glucosidases [19]. Despite the excellent α-glucosidase inhibitory activity in *vitro*, its efficacy in *vivo* was only moderate. Therefore, a large number of DNJ derivatives were prepared in the hope of increasing the in *vivo* activity. The *N*-alkyl derivatives were most effective, and this led to the development of *N*-hydroxyethyldeoxynojirimycin (known as Miglitol or Glyset®) as an oral treatment of the type 2 diabetes with fewer gastrointestinal side effects [14].

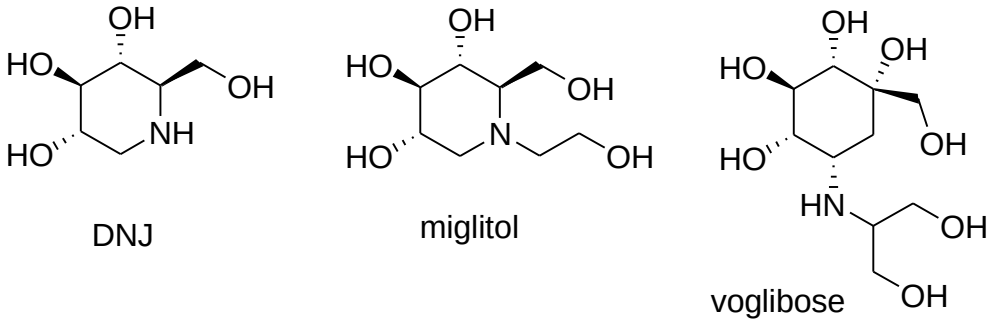


**Figure 1.6** Structures of 1-deoxynojirimycin (DNJ), miglitol and voglibose

Voglibose (Basen®), an *N*-substituted derivative of valiolamine isolated from the fermentation broth of *Streptomyces hygroscopicus*, is a potent and structurally novel inhibitor of the intestinal disaccharidases [20]. Voglibose can be regarded as derivative of 1-deoxynojirimycin (DNJ), which also has a potent inhibitory activity against sucrase and maltase. It has been employed in Japan for the treatment of diabetes since 1994. Voglibose was investigated based on α-glucosidase inhibitory activity; it was shown to be 20 to 30 times more potent than acarbose, thus increasing glucose tolerance by inhibiting its digestion and absorption in the small intestine, especially after meals [21]. The most common adverse effect of voglibose is hepatotoxicity and gastrointestinal disturbance induced by fermentation of unabsorbed carbohydrate in the bowel and increments of gastrointestinal motility [22]. Additionally, the use of voglibose led to less adverse effects including flatulency and abdominal distention, as shown in a random comparative study [14].

In late 1990, salacinol (Figure 1.7) was isolated as a potent α-glucosidases inhibitor from water-soluble extract of the roots and stems of *Salacia reticulata*, which has been traditionally used in India and Sri Lanka for the treatment of diabetes. *Salacia reticulata* Wight, known as kothalahimbutu distributed in Sri Lanka and Indian forests, has been used as a supplementary food in Japan to prevent obesity and diabetes. The mode of action of salacinol was also proved to be the

competitive inhibition against α-glucosidase, and $K_i$ values against maltase, sucrase, and isomaltase were revealed as 3.2, 0.84, and 0.59 mg/mL, respectively. The inhibitory activities toward maltase and sucrase are nearly equal to those of acarbose and that toward isomaltase is much more potent than that of acarbose [23]. Kotalanol, a derivative of 1,2,3-trihydroxy-propyl-salacinol, showed more potent inhibitory activity against sucrase than salacinol and acarbose, which was subsequently developed to diabetic drug that used generally in name Diabosol® [24].

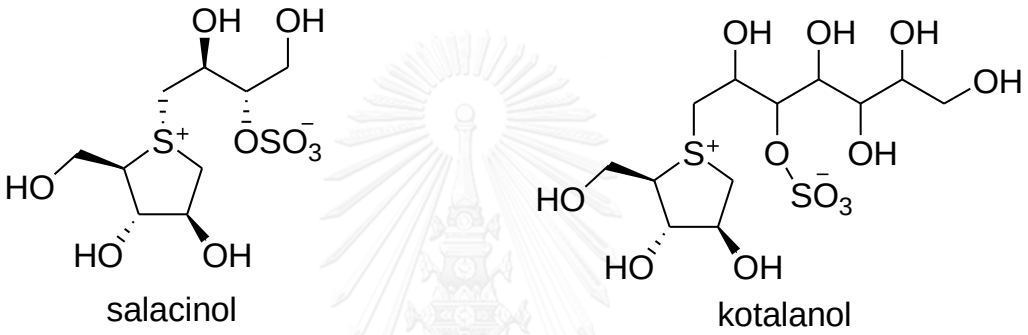


**Figure 1.7** Structures of salacinol and kotalanol



Since antiquity, diabetes has been treated with herb medicines. In Thailand, approximately 200 plants species are employed as antidiabetes agents. Thai Traditional Medicine was long-term mainstream medical system, which has benefit of the healthcare system. In addition, there are many reports showed increasing use of medicinal plants as antidiabetic drugs, in which the studies have been conducted both in human. Therefore, Thai medicinal plants have potential to be used as antidiabetic drugs. In this research, following criterion are adopted for plant seletion.

1. Reducing blood sugar and no toxic in long-term administration
2. Commercially or readily available and use less time in production
3. No report on the use as α-glucosidase inhibitors

### 1.3 *Orthosiphon aristarus* (Blume) Miq.: botanical aspects and literature reviews

*Orthosiphon aristatus* (syn. *O.grandiflorus, O.spicatus* and *O.stamineus*) Figure 1.8 is a perennial herb of the family Lamiaceae and known locally in Malaysia (Misai Kucing), Thailand (Yaa Nuat Maeo), Indonesia (Kumis Kucing or Remujung) as well as throughout Southeast Asia and Australia. It has been used as one of the popular traditional folk medicines in Southeast Asia for the treatment of renal inflammation, kidney stones, and dysuria, and in some areas for diabetes, hypertension, rheumatism, tonsillitis, renal inflammation and menstrual disorder [25, 26]. This plant is one of the most popular medicinal plants used in Thai traditional medicine to treat dysuria [27].

**Figure 1.8** *Orthosiphon aristatus* (Blume) Miq.

In 1991, there have some reports of several caffeic acid depsides, including the main component rosmarinic acid as the predominant phenolic constituents in the leaves of *O. aristatus* as well as in the tea prepared from leafy shoots of this species [28]. In 2010, some research studied the antioxidant and anti-inflammatory agents of *O. aristatus* using the various solvents. According to the results, potent antioxidant activity was observed displayed in the MeOH and EtOH extracts. Furthermore, EtOH extract of this plant also exhibited anti-inflammation [29]. In 2013, Di and coworkers studied the chemical constituents from the aerial parts of *Orthosiphon aristatus* var. *aristatus*. Using 95% EtOH as a solvent, as this research, led to the isolation of nine new compounds diterpenoids (**1-9**), together with 15 previously reported diterpenoids (**10-24**). The known compounds were identified as orthosiphols A (**10**), B (**11**) [30], D (**12**), E (**13**) [31], M (**14**), N (**15**) [32], O (**16**), and Q (**17**) [33], orthosiphonone A (**18**) [34], 7-*O*-deacetylorthosiphol B (**19**), 2-*O*-deacetylorthosiphol J (**20**) [35], neoorthosiphol A (**21**) and B (**22**) [36], secoorthosiphol B (**23**) [37], and norstaminols B (**24**) [38] were isolated from the aerial parts of *O. aristatus* (Figure 1.9). Their structures were established on the basis of extensive spectroscopic analysis. Compounds **13**, **17**, and **23** showed weak inhibitory activity on the proliferation of the SKOV3, DU145, and PC-3 cell lines, respectively [39].

In addition, the hot water extract from leaves of *O. aristatus* was reported to contain two migrated pimarane-type diterpenes, four isopimarane-type diterpenes, three benzochromenes and two flavones. They exhibited suppressive effect on contractile responses in rat thoracic aorta [40].

In this research, the chemical constituents from the twigs and leaves of *O. aristatus* were isolated using polar solvents. The experiments were simulated the same as tea preparation to of this effect have not been identified. Therefore, it is of interest to study the effect of different solvents, extraction methods and plant parts on the $\alpha$-glucosidase inhibition.

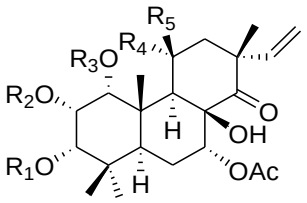

**1** $R_1$=Ac $R_2$=Bz $R_3$=H $R_4$=OBz $R_5$=H
**2** $R_1$=H $R_2$=Bz $R_3$=H $R_4$=OBz $R_5$=H
**3** $R_1$=Bz $R_2$=Bz $R_3$=H $R_4$,$R_5$=O
**5** $R_1$=H $R_2$=Ac $R_3$=Bz $R_4$=OBz $R_5$=H
**6** $R_1$=Ac $R_2$=H $R_3$=Bz $R_4$=OBz $R_5$=H
**7** $R_1$=Bz $R_2$=Ac $R_3$=Bz $R_4$,$R_5$=O

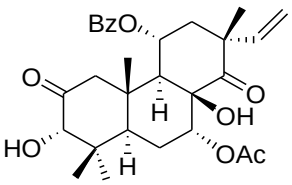

**4**

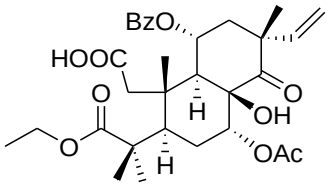

**5**

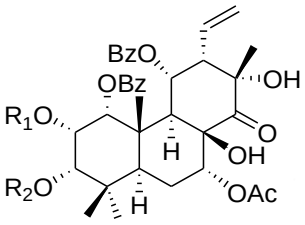

**9** $R_1$,$R_2$=H
**21** $R_1$=H $R_2$=Ac
**22** $R_1$=Bz $R_2$=H

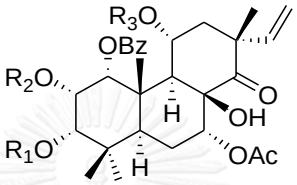

**10** $R_1$=Ac $R_2$=H $R_3$=Bz
**11** $R_1$=H $R_2$=Ac $R_3$=Bz
**16** $R_1$=Bz $R_2$=Ac $R_3$=H

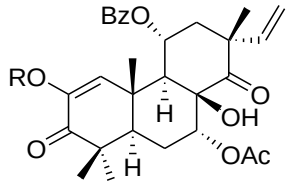

**12** R=Ac
**13** R=H

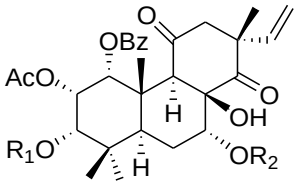

**14** $R_1$=H $R_2$=Ac
**15** $R_1$=Bz $R_2$=H
**18** $R_1$=Bz $R_2$=Ac
**20** $R_1$,$R_2$=H

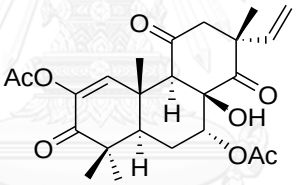

**17**

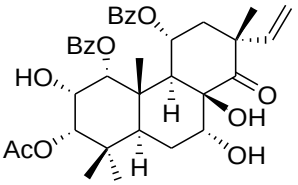

**19**

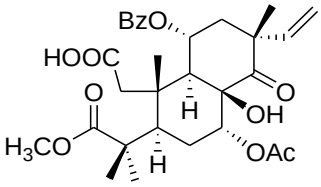

**23**

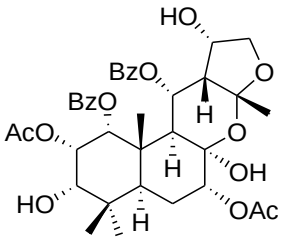

**24**



**Figure 1.9** Structures of all compounds reported by Di and coworkers.

# CHAPTER II

# BIOASSAY-GUIDED ISOLATION AND CHARACTER ISOLATION OF α-GLUCOSIDASE INHIBITORS

## 2.1 Preliminary study on extraction method and plant part

From previous studies conducted by several groups, antidiabetic activity of this plant has been found in different extracts. Therefore, it is difficult to exactly determine which secondary metabolites are the true active components. In this study, we examined α-glucosidase inhibition of leave and twig extracts separately rather than using aerial parts, which usually contain leaves, twings and stems together. In addition, we also hypothesized that extraction method would affect on the enrichment of particular type of secondary metabolites into particular extracts. We therefore designed two different extraction methods (Scheme 2.1) that simulated current use of this plant as herbal remedy for diabetes treatment. Methods 1 and 2 simulated the use of this plant as herbal tea and herbal powder packed in capsule, respectively.

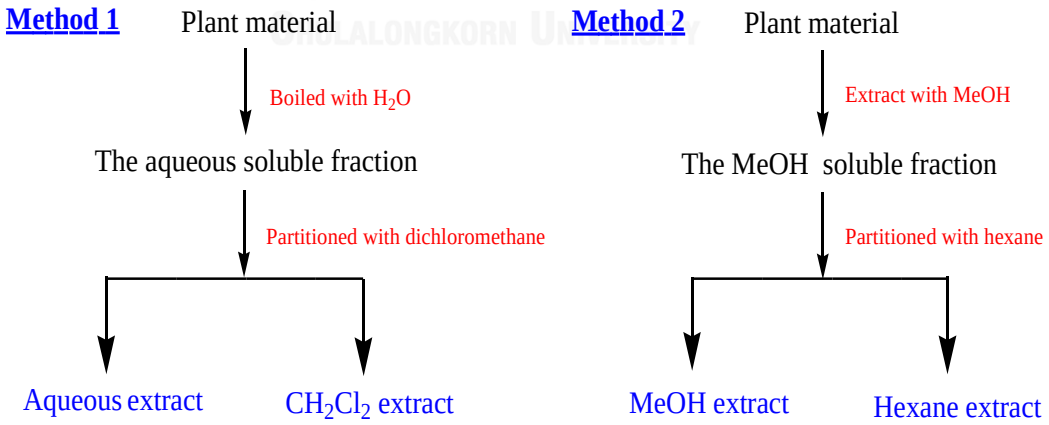


**Scheme 2.1** Extraction methods applied in bioassay screening.

Both methods were applied to prepare extracts from leaves and twigs. The resulting extracts were evaluated for α-glucosidase inhibition (Figure 2.1 and 2.2) against rat intestinal sucrase and maltase.

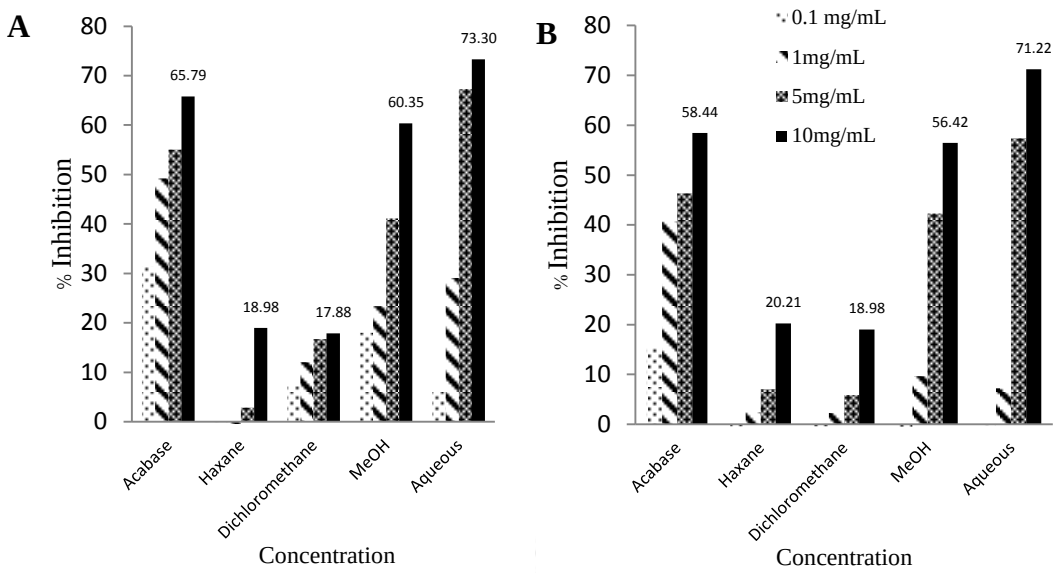


**Figure 2.1** α-Glucosidase inhibitory activity of leaves extracts against sucrase (A) and maltase (B) at concentrations of 0.1-10 mg/mL

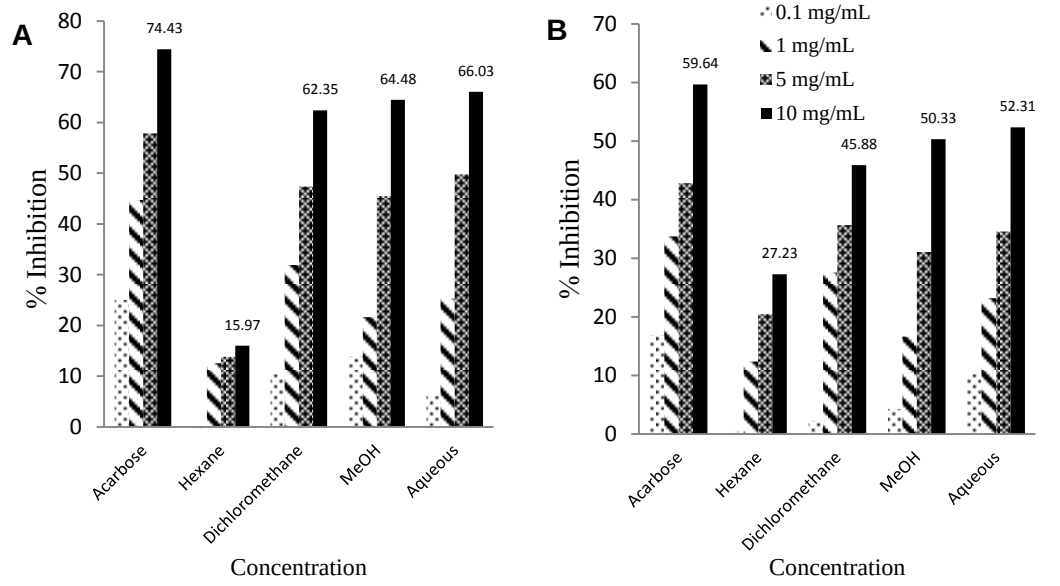


**Figure 2.2** α-Glucosidase inhibitory activity of twigs extracts against sucrase (A) and maltase (B) at concentrations of 0.1-10 mg/mL.

According to Figure 2.1 and 2.2, the aqueous extracts showed the most potent in dose-dependent manner. These result suggested that the extraction methods 1 would be suitable to enrich active components responsible for α-glucosidase inhibition. In addition, the aqueous extract from leaves displayed relatively higher inhibition (71-73%), 10 mg/mL, than those from twigs (52-66%). Therefore, *O. aristatus* leaves were further investigated using the extraction methods 1.

**2.2 Isolation and purification of active components**

Large scale preparation of leave extracts using extraction methods 1 was carried out as follows. Briefly, the air-dried leaves of *O. aristatus* (1000g) were boiled with $H_2O$ at 80-90 °C for 1 hour and cooled down to room temperature. The decoction was partitioned with $CH_2Cl_2$ (3×2L). The aqueous soluble fraction was subjected to Diaion HP-20 column and eluted with $H_2O$ and MeOH, respectively. The fraction (41.36g) eluted with MeOH was subjected to vacuum liquid column chromatography (VLC) over silica gel, to afford methyl caffeate (**1**), 3,4-dihydroxybenzaldehyde (**2**), methyl rosmarinate (**3**) and rosmarinic acid (**4**). The Isolation procedure was summarized in scheme 2.2.

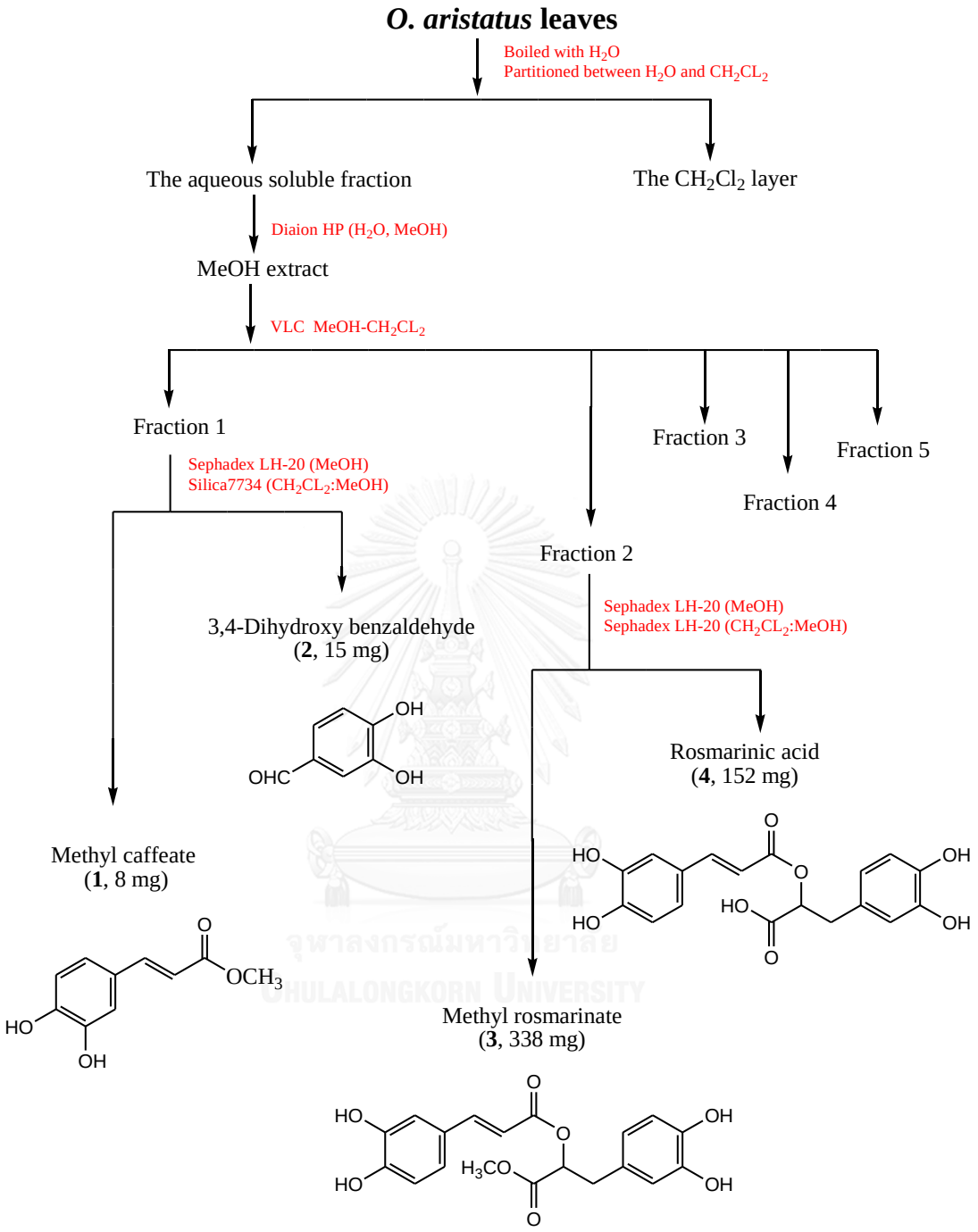


**Scheme 2.2** Isolation procedure

## 2.3 Identification of Isolation components

The isolated compounds from *O. aristatus* were characterized mainly by NMR data as methyl caffeate (**1**), 3,4-dihydroxybenzaldehyde (**2**), methyl rosmarinate (**3**), rosmarinic acid (**4**).

### 2.3.1 Structure elucidation of methyl caffeate (1)

Hydroxycinnamate shows characteristic signals of *trans*-olefin protons (H-7 and H-8) as doublet and α,β-unsaturated ketone (C-9) at $\delta_C$169.9 ppm. Methyl caffeate was obtained as pale yellow oil. The $^{1}$H and $^{13}$C NMR data showed a hydroxycinnamate pattern at 7.45 (d, *J* = 16 Hz, H-7), 6.15 (d, *J* = 16 Hz, H-8) and 169.9 (C-9). An ABX system ($\delta_H$ 6.94, 6.84, and 6.69) of a caffeoyl moiety was also observed. One singlet at $\delta_H$ 3.66 indicated the presence of methoxy group. These spectroscopic data of methyl caffeate were similar to those in a previous report [41].

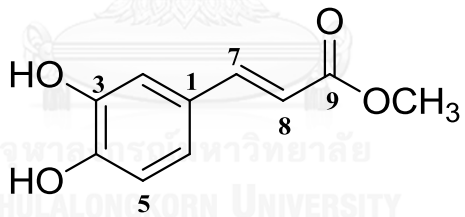


Methyl caffeate (**1**)

### 2.3.2 Structure elucidation of 3,4-dihydroxybenzaldehyde (2)

3,4-Dihydroxybenzaldehyde (**2**) was obtained as a pale yellow oil. An ABX type proton system was observed at $\delta_H$ 7.21, 7.20, and 6.81. Compound **2** also showed a singlet of aldehyde proton at $\delta_H$ 9.59. The $^{13}$C NMR data of **2** displayed characteristic signal of carbonyl of aldehyde group at $\delta_C$ 193.2. These $^{1}$H and $^{13}$C data of **2** were similar to those reported in the literature [42].

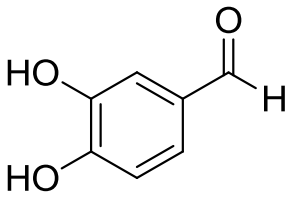


3,4-Dihydroxybenzaldehyde **(2)**

### 2.3.3 Structure elucidation of methyl rosmarinate (3)

Methyl rosmarinate (**3**) was obtained as a white-yellow amorphous solid. The $^{1}$H and $^{13}$C NMR data showed a hydroxycinnamate pattern at 7.46 (d, *J* = 16.0 Hz, H-7), 6.17 (d, *J* = 16 Hz, H-8), and 168.4 (C-9). Compound **3** displayed two resonance clusters of aromatic protons at $\delta_H$ 6.95-6.48 for two ABX type proton systems. In addition, the $^{1}$H NMR data of **3** showed oxygen-bearing methine proton signal at $\delta_H$ 5.09 (H-8'), methylene proton signal at $\delta_H$ 2.94 (H-7'), and methoxy group at $\delta_H$ 3.60. The $^{13}$C NMR data of **3** also displayed characteristic signal of methyl ester group at $\delta_C$ 172.2 (C-9'). These $^{1}$H and $^{13}$C data of **3** were similar to those reported in the literature [43].



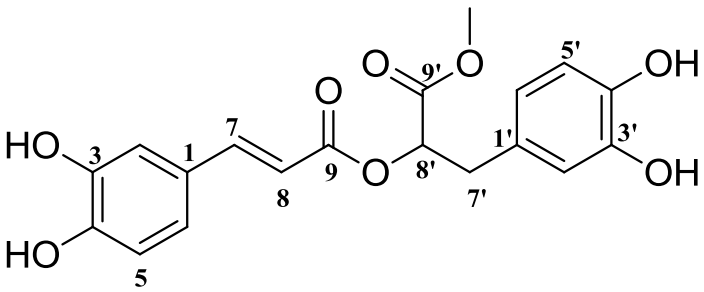


Methyl rosmarinate (**3**)

**2.3.4 Structure elucidation of rosmarinic acid (4)**

Rosmarinic acid (**4**) was obtained as a white-yellow amorphous solid. The $^{1}H$ and $^{13}C$ NMR spectra of **4** showed signals similar to those of **3** and also displayed characteristic signal of carboxylic acid group at $\delta_C$173.6 (C-9'). The NMR data of **4** were similar to those in a previous report [43].

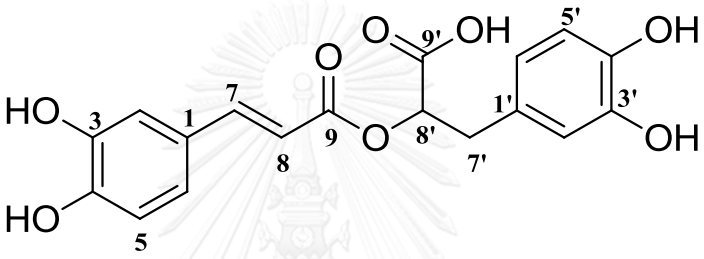


Rosmarinic acid (**4**)

**2.4 Inhibitory activity of compounds 1-4 against α-glucosidases**

α-Glucosidase inhibitory activity of **1-4** are demonstrated in Table 2.1. The isolated compounds **1**, **2**, **3** and **4** from leaves of *O.aristatus* displayed potent α-glucosidase inhibitory activity with $IC_{50}$ values in range of 0.061-0.738 mM.

**Table 2.1** α-Glucosidase inhibitory activity of isolated compounds

| Compounds | α-Glucosidase inhibitory activity ($IC_{50}$,mM)[a] | |
|---|---|---|
| | Maltase | Sucrase |
| Methyl caffeate (**1**) | 0.162±0.041 | 0.124±0.004 |
| 3,4-Dihydroxy benzaldehyde (**2**) | 0.738±0.106 | 0.132±0.028 |
| Methyl rosmarinate (**3**) | 0.081±0.047 | 0.067±0.017 |
| Rosmarinic acid (**4**) | 0.249±0.114 | 0.061±0.011 |
| Acarbose[b] | 0.132±0.131 | 0.074±0.013 |

[a] The $IC_{50}$ value is defined as the inhibitor concentration to inhibit 50% of enzyme activity (mM).
[b] Standard control

The inhibitory effects of **1-4** against rat intestine α-glucosidase were examined (Table 2.1). Apparently, methyl rosmarinate (**3**) showed highly potent inhibition against maltase with $IC_{50}$ value of 0.081 mM. However, methyl rosmarinate (**3**) and rosmarinic acid (**4**) displayed comparable inhibition against sucrase with $IC_{50}$ values of 0.067 and 0.061mM, respectively. However, compounds **1** and **2** revealed slightly weaker inhibition than compounds **3** and **4**.

Previous study indicated that methyl rosmarinate (**3**) and rosmarinic acid (**4**) inhibited α-glucosidase in baker' yeast. The inhibitory effects of phenolics from *R. serra* on yeast α-glucosidase assayed at different concentrations. Enzymatic activity decreased mildly when the concentration of compound **3** and **4** increased from 0 to 0.4 mM, the remaining activity was 71.5% and 87.0% of the initial activity [44]. This result related with our research which showed high potent activity in both enzymes.

## 2.5 Experimental section

### 2.5.1 General experiment procedures

The $^{1}H$ and $^{13}C$ NMR spectra ($CD_3OD$) were recorded with a nuclear magnetic resonance spectrometer of Varian model Mercury$^{+}$ 400. The chemical shift in $\delta$ (ppm) was assigned with reference to the signal from the residual protons in deuterated solvents. Sephadex LH-20 and silica gel 60 Merck cat. No. 7734 and 7729 were used for open column chromatography. Thin layer chromatography (TLC) was performed on precoated Merck silica gel 60 $F_{254}$ plates (0.25 mm thick layer).

### 2.5.2 Plant material

The whole plant of *O. aristatus* was collected from Chonburi, Thailand in April 2012. The specimen (BCU-A014171) was authenticated by the botanist (Parinyanoot Klinratana) and deposited at Department of Botany, Chulalongkorn University.

### 2.5.3 Extraction and isolation

The air-dried leaves of *O. aristatus* (1000 g) were boiled with $H_2O$ at 80-90 °C for 1 hour and cooled down to room temperature. The decoction was partitioned with $CH_2Cl_2$ (3×2L). The aqueous soluble fraction was subjected to Diaion HP-20 column and eluted with $H_2O$ and MeOH, respectively. The combined fractions (41.36 g) eluted with MeOH were subjected to vacuum liquid column chromatography (VLC) over silica gel, which were eluted with (each 500 mL) $CH_2Cl_2$, MeOH/$CH_2Cl_2$ (10:90), MeOH/$CH_2Cl_2$ (20:80), MeOH/$CH_2Cl_2$ (40:60) and 100% MeOH, respectively, yielding totally 5 fractions (Or13-1 to Or13-5). Fraction Or13-1 was applied over Sephadex LH-20 eluted with MeOH to yield 4 subfractions (Or15-1 to Or15-4). Subfraction Or15-4 was purified by silica gel using MeOH/$CH_2Cl_2$ (40:60) and 100% MeOH to yield 6 subfractions (Or17-1 to 17-6). Subfraction Or17-4 afforded methyl caffeate (**1**, 8.4 mg). Subfraction Or17-6 yielded 3,4-dihydroxy benzaldehyde (**2**, 15.7 mg). Fraction Or13-2 was applied over Sephadex LH-20 eluted with MeOH to yield 3 subfractions (Or22-1

to Or22-3). Subfraction Or22-2 was further purified by Sephadex LH-20 using MeOH/$CH_2Cl_2$ (10:90) and 100% MeOH to yield 4 subfractions (Or23-1 to Or23-7). Subfraction Or23-4 afforded methyl rosmarinate (**3**, 338.4 mg). Subfraction Or23-7 was purified by Sephadex LH-20 column using MeOH/$CH_2Cl_2$ (10:90) MeOH/$CH_2Cl_2$ (20:80) and MeOH to yield 4 subfractions (Or28-1 to Or28-5), in which subfraction Or28-3 afforded rosmarinic acid (**4**, 152 mg).

**Methyl caffeate** (**1**): $^1$H NMR ($CD_3OD$, 400 MHz ) $\delta$ 7.45 (1H, d, *J*=16 Hz, H-7), 6.94 (1H, d, *J*=1.6 Hz, H-2), 6.84 (1H, dd, *J*=1.6, 8 Hz, H-6), 6.69 (1H, d, *J*=8 Hz, H-5), 6.15 (1H, d, *J*=16 Hz, H-8), 3.66 (3H, s, $OCH_3$); $^{13}$C NMR ($CD_3OD$, 100 MHz) $\delta$ 169.9, 149.5, 147.0,146.9, 127.7, 122.9, 116.6, 114.9,114.9, 52.1.

**3,4-Dihydroxybenzaldehyde** (**2**): $^1$HNMR ($CD_3OD$, 400MHz) $\delta$ 9.59 (1H, s, CHO), 7.21 (1H, dd, *J*=8.8, 2 Hz), 7.20 (1H, s), 6.81 (1H, d, *J*=8 Hz); $^{13}$C NMR ($CD_3OD$, 100 MHz) $\delta$ 193.2, 153.7, 147.1, 130.7, 126.5, 115.7, 114.9.

**Methyl rosmarinate** (**3**): $^1$H NMR ($CD_3OD$, 400 MHz) $\delta$ 7.46 (1H, d, *J*=16 Hz, H-7), 6.95 (1H, d, *J*=1.6 Hz, H-2), 6.86 (1H, dd, *J*=8.4, 2 Hz, H-6), 6.69 (1H, d, *J*=8 Hz, H-5), 6.61 (1H, s, H-5'), 6.60 (1H, d, *J*=8 Hz, H-2'), 6.48 (1H, dd, *J*=8, 4 Hz, H-6'), 6.17 (1H, d, *J*=16 Hz, H-8), 5.09 (1H, dd, *J*=8, 4 Hz, H-8'), 3.60 (3H, s, -OMe), 2.94 (2H, d, *J*=8, 4 Hz, H-7'); $^{13}$C NMR ($CD_3OD$, 100 MHz) $\delta$ 172.2, 168.4, 149.8, 148.0, 146.8, 146.2, 145.4, 128.8, 127.6, 123.2, 121.8, 117.6, 116.6, 116.4, 115.3, 114.2, 74.7, 52.7, 37.9.

**Rosmarinic acid** (**4**): $^1$H NMR ($CD_3OD$, 400 MHz) $\delta$ 7.55 (1H, d, *J*=15.9 Hz, H-7), 7.04 (1H, d, *J*=2.2 Hz, H-2), 6.94 (1H, dd, *J*=8.6, 2.1 Hz, H-6), 6.77 (2H, m, H-5,2'), 6.70 (1H, d, *J*=8 Hz, H-5'), 6.61 (1H, dd, *J*=8.1, 2.1 Hz, H-6'), 6.26 (1H, d, *J*=16 Hz, H-8), 5.19 (1H, dd, *J*=8.1, 4.3 Hz, H-8'), 3.05 (2H, m, H-7); $^{13}$C NMR ($CD_3OD$, 100 MHz) $\delta$ 173.6, 168.6, 149.7, 147.8, 146.8, 146.2, 145.3, 129.4, 127.8, 123.2, 122.0, 117.7, 116.6, 116.5, 115.4, 114.5, 74.7, 37.9

### 2.5.4 α-Glucosidase inhibitory activity

#### 2.5.4.1 Chemical and equipment

The α-glucosidase (EC 3.2.1.20) from rat intestine and substrates (maltose and sucrose) were supplied by Sigma Aldrich Co. (USA). Glu-kit was purchased from Human Gesellschaftfür Biochemicaund DiagnosticambH (Germany). The crude enzyme solution prepared from rat intestinal acetone powder was used as a source of maltase (0.45 U/mg proteins) and sucrase (0.09 U/mg proteins). Rat intestinal acetone powder (1.0 g) was resuspended in 30 mL of 0.9% NaCl solution. After centrifugation (12,000*g*, 30 min), the supernatant was used for the assay. Acarbose (Glucobay® 50 N 1; Bayer Vital, Leverkusen, Germany) was used as a synthetic inhibitor of α-glucosidase. Bio-Radmicroplate reader model 3550 UV was used to measure the absorbance at 503 nm for the enzyme reaction in the microplate assay.

#### 2.5.4.2 α-Glucosidase inhibitory activity from rat intestinal

The enzymatic hydrolysis of the maltose and sucrose were monitored based on the amount of glucose released. The concentration of glucose released from the reaction mixture was determined by the glucose oxidase (GOD) method using a glu-kit (Human, Germany). The reaction between hydrogen peroxide and 4-aminphenazone together with phenol under peroxidase (POD) yieldeda red-violet quinoneimine dye as indicator. Enzymatic activity was quantified by measuring absorbance of quinoneimine at 503 nm (Scheme 2.5).

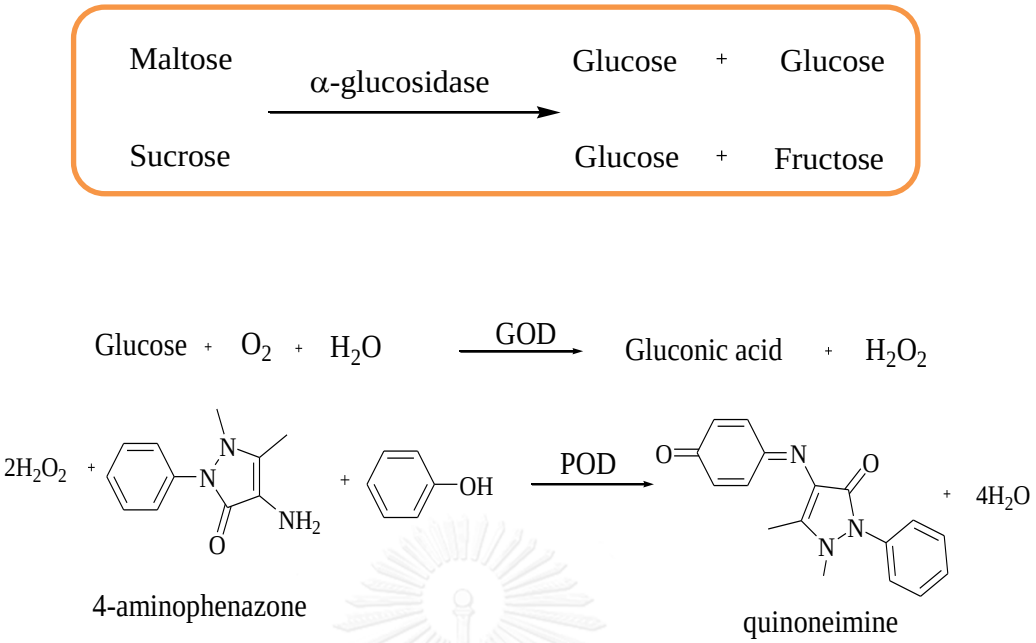


**Scheme 2.3** Hydrolysis of maltose and sucrose by rat intestinal α-glucosidases.



**Procedure**

Assay was performed according to the method described by Jo and coworkers with slight modification. In the 96-well plate, 10 µL of sample (0.1, 1, 5 and 10 mg/mL in DMSO) was added with 30 µL of the 0.1 M phosphate buffer (pH 6.9), 20 µL of the substrate solution (maltose: 10 mM; sucrose: 100 mM) in 0.1 M phosphate buffer, 80 µL of glucose kit and 20 µL of the crude enzyme solution. The reaction mixture was then incubated at 37 °C for 10 min (for maltose) and 40 min (for sucrose). The concentration of glucose released from the reaction mixture was determined by the glucoseoxidase method using a commercial glucose assay kit (Human, Germany). Acarbose® was used as a positive control in this assay. Enzymatic activity was quantified by measuring absorbance at 503 nm. The percentage inhibition and $IC_{50}$ value are calculated as follows

$$\% \text{ inhibition} = [(A_0 - A_1)/A_0] \times 100$$

Where, $A_0$ is the absorbance without the sample, and $A_1$ is the absorbance with the sample. The $IC_{50}$ value was determined from a plot of percentage inhibition versus sample concentration.

# CHAPTER III

# KINETIC MECHANISM OF INHIBITORY

## 3.1 Evaluation of kinetic mechanism

The kinetic analysis of methyl rosmarinate (**3**) and rosmarinic acid (**4**) were estimated in the previous report [44]. Methyl rosmarinate (**3**) showed mixed-type inhibition while rosmarinic acid (**4**) was found to be a competitive inhibitor against yeast α-glucosidase. However, there is still no report on kinetic analysis against rat intestinal α-glucosidase. The kinetic analysis in rat intestinal (sucrase and maltase) were carried out using Lineweaver-Burk plots. Type of inhibition could be determined by analyzing Lineweaver-Burk plots, $K_m$ and $V_{max}$ (Table 3.1)

**Table 3.1** Inhibition mechanism

| Type of inhibition | $K_m$ | $V_{max}$ | Intersection |
|---|---|---|---|
| Competitive | increase | unchanged | Y axis, Y>0 |
| Non-competitive | unchange | decrease | X axis, X<0 |
| Uncompetitive | decrease | decrease | no intersection |
| Mixed | increase | decrease | second quadrant |

### 3.1.1. Kinetic mechanism underlying the inhibition of methyl rosmarinate (3) against rat intestinal glucosidases

The kinetic analysis against rat intestinal sucrase and maltase was carried out using Lineweaver-Burk plots. Methyl rosmarinate (**3**) showed a series of straight lines with increasing $K_m$ and decrease $V_{max}$ values; all of which intersected in the second quadrant (Figure 3.1). This behaviour indicated that mix-type inhibition of **3** against in sucrase.

In other words, methyl rosmarinate (**3**) could inhibited sucrase by two different pathway, competitive and noncompetitive manners. To further study the pathway in

which compound **3** preferentially inhibited sucrase, the dissociation constants $K_i$ (for EI complex) and $K_i'$ (for ESI complex) were determined. The secondary plot between slope and inhibitor concentration (Figure 3.2) indicated the $K_i$ values of 0.011 mM whereas the plot between intercept and inhibitor concentration (Figure 3.3) suggested the $K_i'$ values of 0.2 mM. The small $K_i$ values indicated that the inhibitor preferentially bind to the enzyme in competitive manner rather than form ESI complex in noncompetitive manner.

The kinetic mechanism of **3** against maltase was also investigated. Apparently, methyl rosmarinate (**3**) also inhibited maltase by mix-type inhibition (Figure 3.4). In addition, the smaller value of $K_i$ (Figure 3.5) than $K_i'$ (Figure 3.6) implied the inhibition of **3** against maltase was dominant in competitive manner. The kinetic parameters of methyl rosmarinate (**3**) were summarized in Table 3.2.

**Table 3.2** Kinetic parameters of methyl rosmarinate (**3**)

| **α-Glucosidase inhibition** | **Type of inhibition** | $K_i$ | $K_i'$ | $K_m$ |
|---|---|---|---|---|
| Sucrase | Mixed | 0.011 mM | 0.2 mM | 1.61 |
| Maltase | Mixed | 0.045 mM | 0.054 mM | 3.94 |

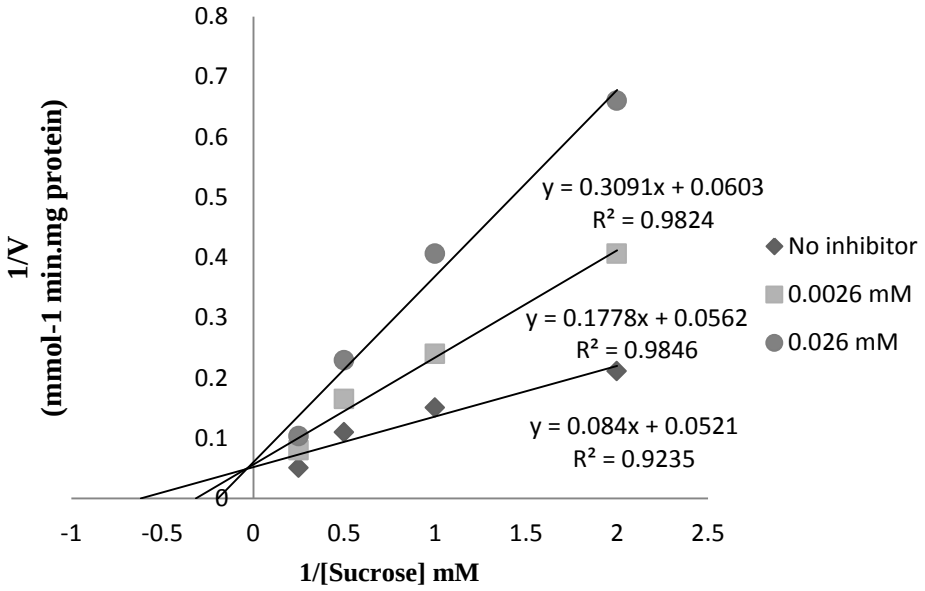


**Figure 3.1** Lineweaver-Burk plot for inhibitory activity of methyl rosmarinate (**3**) against intestinal sucrase.

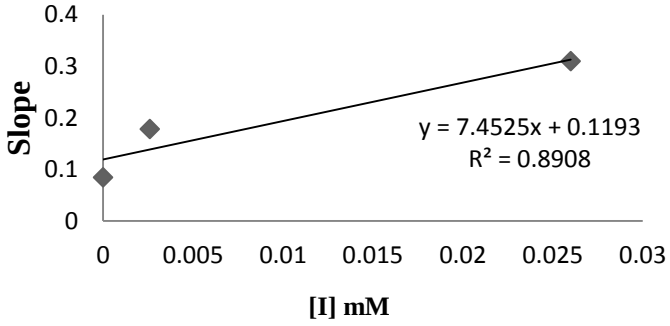


**Figure 3.2** Secondary plot of slope vs. [I] from a Lineweaver-Burk plot for the determination of $K_i$

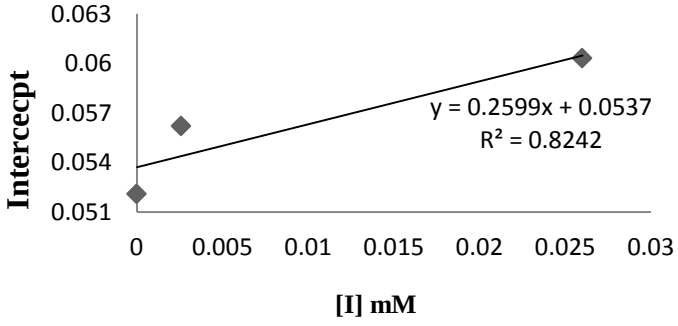


**Figure 3.3** Secondary plot of intercept vs. [I] from a Lineweaver-Burk plot for the determination of $K_i'$

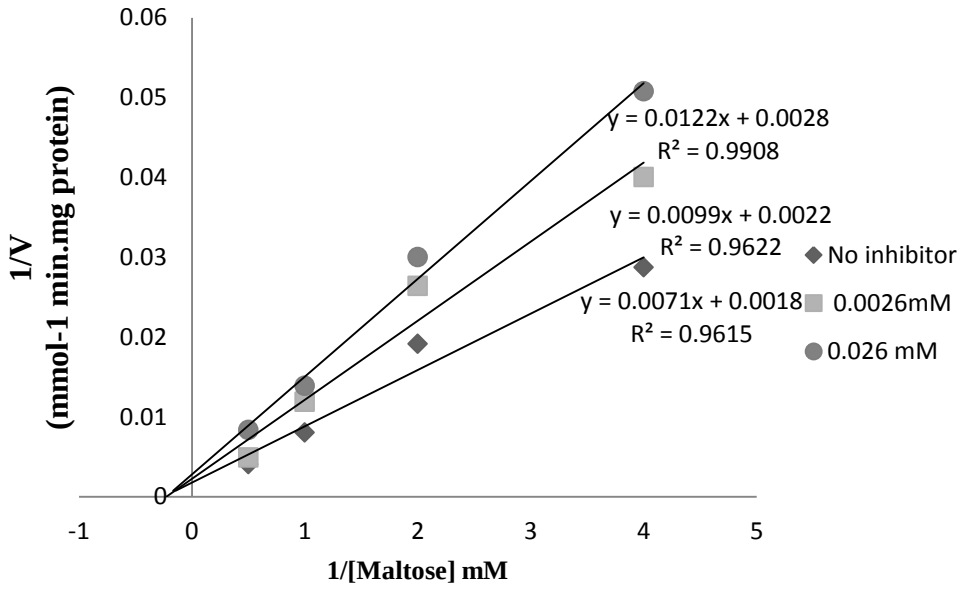


**Figure 3.4** Lineweaver-Burk plot for inhibitory activity of methyl rosmarinate (**3**) against intestinal maltase.

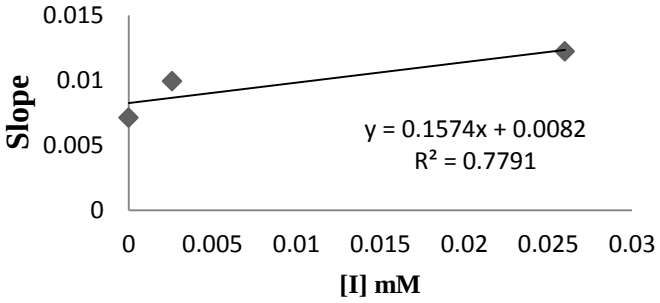


**Figure 3.5** Secondary plot of slope vs. [I] from a Lineweaver-Burk plot for the determination of $K_i$

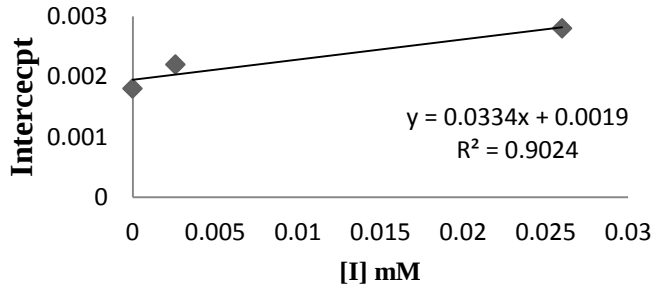


**Figure 3.6** Secondary plot of intercept vs. [I] from a Lineweaver-Burk plot for the determination of $K_i'$

### 3.1.2. Kinetic mechanism underlying the inhibition of rosmarinic acid (4) against rat intestinal glucosidases

The kinetic analysis against rat intestinal sucrase and maltase was carried out using aforementioned methods. The Lineweaver-Burk plot (Figure 3.7) of rosmarinic acid (**4**) showed a series of straight lines which intersect y axis at the some position. These lines showed increased $K_m$ while $V_{max}$ unchanged. This behavior indicated competitive manner of rosmarinic acid (**4**) toward sucrase with $K_i$ value of 0.013 mM (Figure 3.8).

On the contrary, Compound 4 showed mixed type inhibition (Figure 3.9) because intersection of each rosmarinic acid concentration line showed in second quadrant. The data of $K_m$ and $V_{max}$ analysis were consistent with those of mixed type inhibition (Table 3.1). Mix type inhibition has both $K_i$ and $K_i'$ values. $K_i$ value was investigated though secondary plot of slope vs. [I] from a primary Lineweaver-Burk plot (Figure 3.10). The $K_i'$ show affinity of inhibitor to enzyme-substrate complex (**ES**) and obtained by plotting between secondary plot of intercept *vs*. [I] from a primary Lineweaver-Burk plot (Figure 3.11). Dissociation constants of $K_i$ (0.04 mM) and $K_i'$ (0.09mM) values were compared. It was found that the $K_i$ value was less than $K_i'$ value two times (Table 3.3), suggesting that binding affinity of rosmarinic acid to free enzyme (**E**) stronger than enzyme-substrate complex (**ES**). The data implied that rosmarinic acid is dominant in competitive inhibition**.**



**Table 3.3** Kinetic parameters of rosmarinic acid (**4**)

| **α-Glucosidase inhibition** | **Type of inhibition** | $K_i$ | $K_i'$ | $K_m$ |
|---|---|---|---|---|
| **Sucrase** | Competitive | 0.013 mM | - | 1.23 |
| **Maltase** | Mixed | 0.04 mM | 0.09 mM | 2.85 |

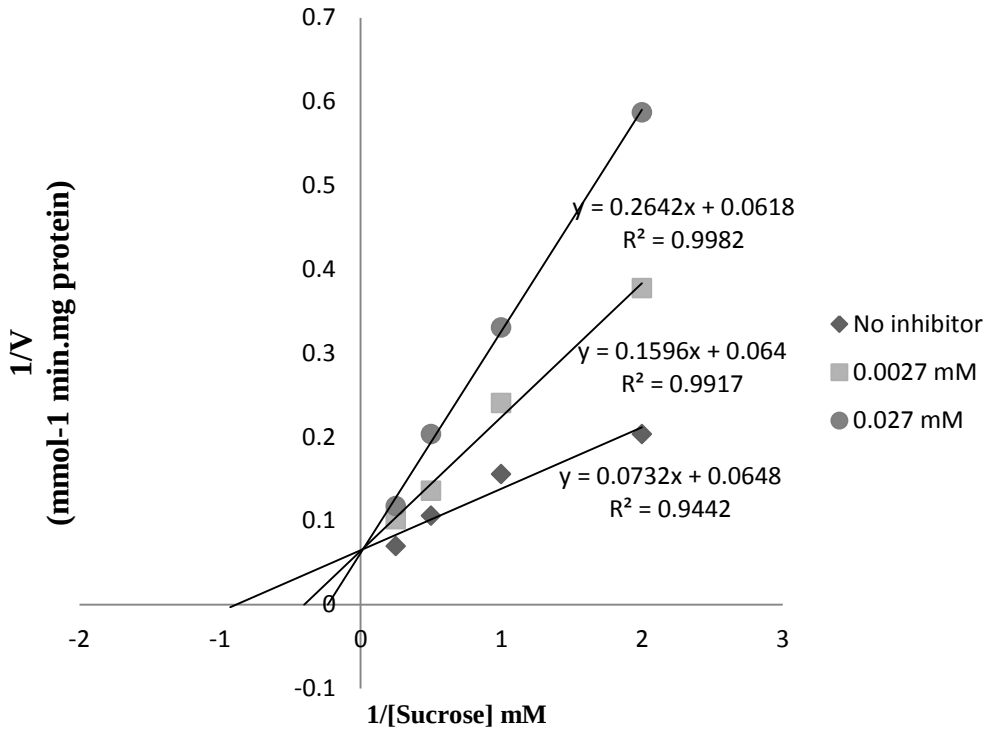


**Figure 3.7** Lineweaver-Burk plot for inhibitory activity of rosmarinicacid (**4**) against intestinal sucrase.

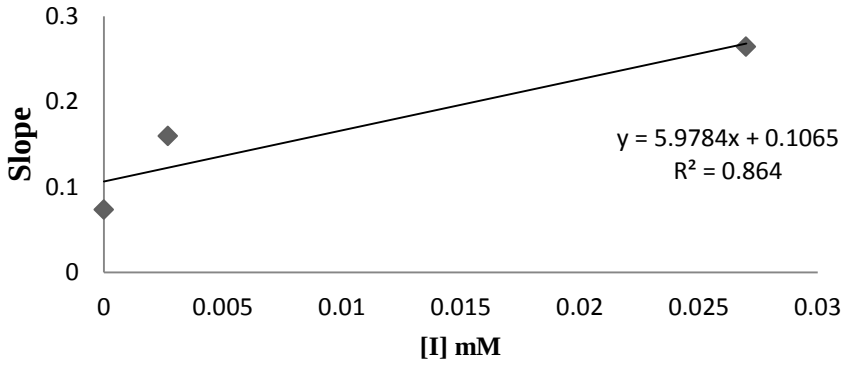


**Figure 3.8** Secondary plot of slope *vs*. [I] from a Lineweaver-Burk plot for the determination of $K_i$

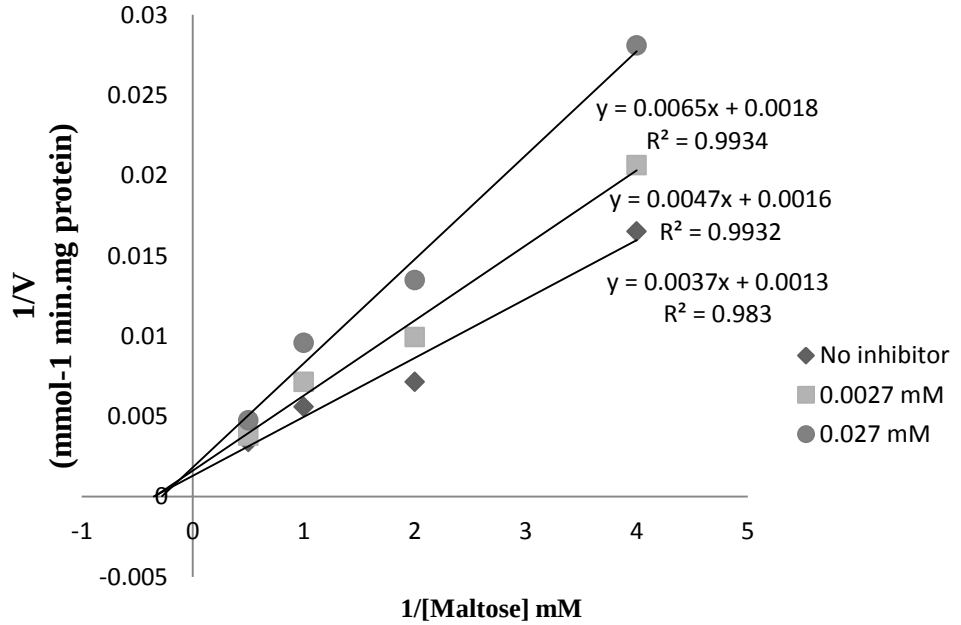


**Figure 3.9** Lineweaver-Burk plot for inhibitory activity of rosmarinic acid (**4**) against intestinal maltase.

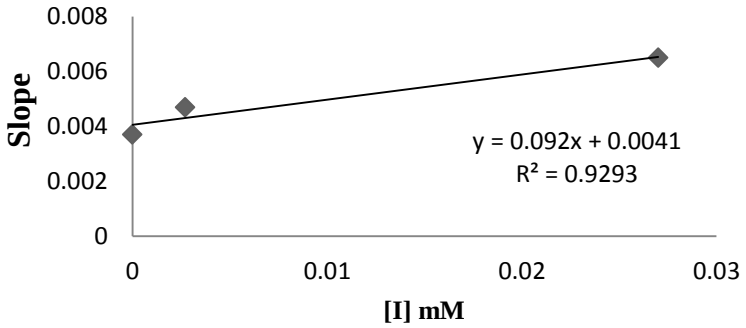


**Figure 3.10** Secondary plot of slope *vs*. [I] from a Lineweaver-Burk plot for the determination of $K_i$

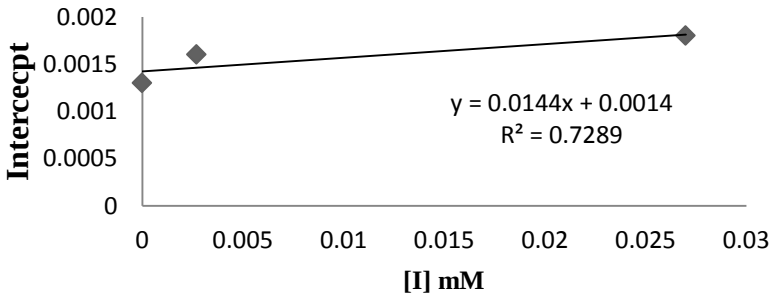


**Figure 3.11** Secondary plot of intercept *vs*. [I] from a Lineweaver-Burk plot for the determination of $K_i'$

## 3.2 Experimental section

### 3.2.1 Measurement of kinetic constant

For kinetic analyses of rat **α**-glucosidase (maltase and sucrase) by the active compounds (**3** and **4**), enzyme and active compounds were incubated with increasing concentrations of maltose (0.5-20 mM) and sucrose (5-200 mM). The type of inhibition was determined by Lineweaver-Burk plot whereas the $K_i$ and $K'_i$ values were deduced from the secondary plots of slope *vs* [I] and the interception *vs* [I] of the Lineweaver-Burk plots, respectively.

# CHAPTER IV
# CONCLUSION

Crude extracts from leaves and twigs of *O. aristatus* which prepared by two different extraction methods-decoction and maceration were screened for α-glucosidase inhibition. Apparently, the leave extract prepared by decoction with hot water showed more potent inhibition. The aqueous extracts showed the most potent in dose-dependent manner. These result suggested that the extraction methods would be suitable to enrich active components responsible for α-glucosidase inhibition. In addition, the aqueous extract from leaves displayed relatively higher inhibition (71-73%), 10 mg/mL, than those from twigs (52-66%). Bioassay-guided fractionation of the aqueous extract from leaves led to the isolation of methyl caffeate (**1**), 3,4-dihydroxy benzaldehyde (**2**), methyl rosmarinate (**3**) and rosmarinic acid (**4**). Compounds **1** and **2** were isolated from fraction 1, while, compounds **3** and **4** were purified from the fraction 2. The isolated compounds inhibited maltase and sucrase with $IC_{50}$ value in the range of 0.061-0.738 mM, which are equipotent to standard antidiabetic drug acarbose. The compounds **3** and **4** expressed the good potent on rat intestinal glucosidases, thus, these compounds were selected for study the kinetic of the enzyme. The kinetic investigation revealed that maltase was inhibited by methyl rosmarinate and rosmarinic acid through mixed-type whereas sucrase was inhibited through mixed-type and competitive manners.

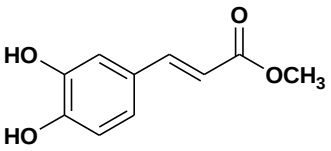


**methyl caffeate (1)**

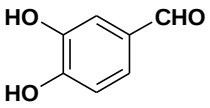


**3,4-dihydroxy benzaldehyde (2)**

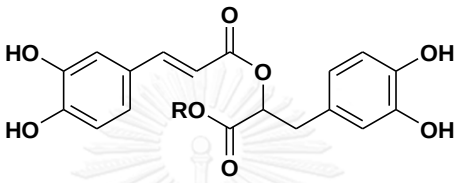


**methyl rosmarinate (3); R = $CH_3$**
**rosmarinic acid (4); R = H**

**Figure 4.1** The chemical structures of isolated compounds from *O. aristatus* leaves 1-4

## REFERENCES


[1] Wild, S., Roglic, G., Green, A., Sicree, R., and King, H. Global prevalence of diabetes: estimates for the year 2000 and projections for 2030. Diabetes Care 27(5) (2004): 1047-1053.

[2] Green, A., Hirsch, N.C., and Pramming, S.K. The changing world demography of type 2 diabetes. Diabetes/Metabolism Research and Reviews 19(1) (2003): 3-7.

[3] Diamond, J. The double puzzle of diabetes. Nature 423(6940) (2003): 599-602.

[4] Skyler, J.S. Diabetes mellitus: Pathogenesis and treatment strategies. Journal of Medicinal Chemistry 47(17) (2004): 4113-4117.

[5] Sharma, D.K., Pandey, J., Tamrakar, A.K., and Mukherjee, D. Synthesis of heteroaryl/aryl kojic acid conjugates as stimulators of glucose uptake by GLUT4 translocation. European Journal of Medicinal Chemistry 85(0) (2014): 727-736.

[6] Chaudhuri, A. and Dandona, P. Effects of insulin and other antihyperglycaemic agents on lipid profiles of patients with diabetes. Diabetes, Obesity and Metabolism 13(10) (2011): 869-879.

[7] Tuomi, T. Type 1 and type 2 diabetes: What do they have in common? Diabetes 54(SUPPL. 2) (2005): S40-S45.

[8] Costanian, C., Bennett, K., Hwalla, N., Assaad, S., and Sibai, A.M. Prevalence, correlates and management of type 2 diabetes mellitus in Lebanon: Findings from a national population-based study. Diabetes Research and Clinical Practice 105(3): 408-415.

[9] Fava, S. Role of postprandial hyperglycemia in cardiovascular disease. Expert Review of Cardiovascular Therapy 6(6) (2008): 859-872.

[10] Krentz, A.J. and Bailey, C.J. Oral antidiabetic agents: Current role in type 2 diabetes mellitus. Drugs 65(3) (2005): 385-411.

[11] Krentz, A.J. and Bailey, C.J. Oral antidiabetic agents current role in type 2 diabetes mellitus. Drugs 2005 65(3) (2005): 385-411.

[12] Xu, H. Inhibition kinetics of flavonoids on yeast α-glucosidase merged with docking simulations. Protein and Peptide Letters 17(10) (2010): 1270-1279.

[13] Rabasa-Lhoret, R. and Chiasson, J.-L. α-Glucosidase Inhibitors. in International Textbook of Diabetes Mellitus: John Wiley & Sons, Ltd, 2003.

[14] Borges de Melo, E., da Silveira Gomes, A., and Carvalho, I. α- and β-Glucosidase inhibitors: chemical structure and biological activity. Tetrahedron 62(44) (2006): 10277-10302.

[15] Horne, G., Wilson, F.X., Tinsley, J., Williams, D.H., and Storer, R. Iminosugars past, present and future: Medicines for tomorrow. Drug Discovery Today 16(3-4) (2011): 107-118.

[16] Li, W.L., Zheng, H.C., Bukuru, J., and De Kimpe, N. Natural medicines used in the traditional Chinese medical system for therapy of diabetes mellitus. Journal of Ethnopharmacology 92(1) (2004): 1-21.

[17] Chen, H., Feng, R., Guo, Y., Sun, L., and Jiang, J. Hypoglycemic effects of aqueous extract of *Rhizoma odorati* in mice and rats. Journal of Ethnopharmacology 74(3) (2001): 225-229.

[18] Yagi, M., Kouno, T., Aoyagi, Y., and Murai, H. The structure of molanoline, a piperidine alkaloid from *Morus* species. Nippon Nogei Kagaku Kaishi 50 (1976): 571-572.

[19] Schmidt, D.D., Frommer, W., Müller, L., and Truscheit, E. Glucosidase inhibitors from bacilli. Naturwissenshaften 66 (1979): 584-585.

[20] Luo, H., Imoto, T., and Hiji, Y. Inhibitory effect of voglibose and gymnemic acid on maltose absorption *in vivo*. World Journal of Gastroenterology 7(2) (2001): 270-274.

[21] Yasuda, K., et al. Long-term therapeutic effects of voglibose, a potent intestinal alpha-glucosidase inhibitor, in spontaneous diabetic GK rats. Diabetes Research and Clinical Practice 59(2) (2003): 113-122.

[22] Nakamura, T., et al. Effect of an α-glucosidase inhibitor on intestinal fermentation and faecal lipids in diabetic patients. Journal of International Medical Research 21(5) (1993): 257-267.

[23] Yoshikawa, M., et al. Salacinol, potent antidiabetic principle with unique thiosugar sulfonium sulfate structure from the ayurvedic traditional medicine *Salacia reticulata* in Sri Lanka and India. Tetrahedron Letters 38(48) (1997): 8367-8370.

[24] Yoshikawa, M., Murakami, T., Yashiro, K., and Matsuda, H. Kotalanol, a potent **α**-glucosidase inhibitor with thiosugar sulfonium sulfate structure, from antidiabetic Ayurvedic medicine *Salacia reticulata.* Chemical and Pharmaceutical Bulletin 46(8) (1998): 1339-1340.

[25] Bwin, D.M. and Gwan, U.S. In Burmese indegenous medicinal plants: 1. Plants with reputed hypoglycemic action. Health and Myanmar Traditional Medicine. Burma Medical Reasearch Institute, Ministry of Health, Yangon. (1967): 126-128.

[26] kasahara, Y.S. Medicinal herb index in Indonesia. P.T. Esai, Indonesia. (1995): 263-269.

[27] Ngamrojanavanich, N., Manakit, S., Pornpakakul, S., and Petsom, A. Inhibitory effects of selected Thai medicinal plants on $Na^{+}$,$K^{+}$-ATPase. Fitoterapia 77(6) (2006): 481-483.

[28] Sumaryono, W., Proksch, P., Hartmann, T., Nimtz, M., and Wray, V. Induction of rosmarinic acid accumulation in cell suspension cultures of *Orthosiphon aristatus* after treatment with yeast extract. Phytochemistry 30(10) (1991): 3267-3271.

[29] Hsu, C.-L., Hong, B.-H., Yu, Y.-S., and Yen, G.-C. Antioxidant and anti-inflammatory effects of *Orthosiphon aristatus* and its bioactive compounds. Journal of Agricultural and Food Chemistry 58(4) (2010): 2150-2156.

[30] Masuda, T., Masuda, K., Shiragami, S., Jitoe, A., and Nakatani, N. Orthosiphol A and B, novel diterpenoid inhibitors of TPA (12-O-tetradecanoylphorbol-13-acetate)-induced inflammation, from *Orthosiphon stamineus.* Tetrahedron 48(33) (1992): 6787-6792.

[31] Takeda, Y., Matsumoto, T., and Terao, H. Orthosiphol D and E, minor diterpenes from *Orthosiphon stamineus.* Phytochemistry 33(2) (1993): 411-415.

[32] Awale, S., Tezuka, Y., Banskota, A.H., Kouda, K., Tun, K.M., and Kadota, S. Five novel highly oxygenated diterpenes of *Orthosiphon stamineus* from Myanmar. Journal of Natural Products 64(5) (2001): 592-596.

[33] Awale, S., Tezuka, Y., Banskota, A.H., Kouda, K., Kyaw, M.T., and Kadota, S. Four highly oxygenated isopimarane-type diterpenes of *Orthosiphon stamineus*. Planta Medica 68(3) (2002): 286-288.

[34] Shibuya, H., Bohgaki, T., Matsubara, T., Watarai, M., Ohashi, K., and Kitagawa, I. Indonesian medicinal plants. XXII. Chemical structures of two new isopimarane-type diterpenes, orthosiphonones A and B, and a new benzochromene, orthochromene A from the leaves of *Orthosiphon aristatus* (Lamiaceae). Chemical and Pharmaceutical Bulletin 47(5) (1999): 695-698.

[35] Awale, S., Tezuka, Y., Banskota, A.H., Adnyana, I.K., and Kadota, S. Highly-oxygenated isopimarane-type diterpenes from *Orthosiphon stamineus* of Indonesia and their nitric oxide inhibitory activity. Chemical & Pharmaceutical Bulletin 51(3) (2003): 268-275.

[36] Shibuya, H., Bohgaki, T., and Ohashi, K. Two novel migrated pimarane-type diterpenes, neoorthosiphols A and B, from the leaves of *Orthosiphon aristatus* (Lamiaceae). Chemical and Pharmaceutical Bulletin 47(6) (1999): 911-912.

[37] Awale, S., Tezuka, Y., Shimoji, S., Taira, K., and Kadota, S. Secoorthosiphols A-C: Three highly oxygenated secoisopimarane-type diterpenes from Orthosiphon stamineus. Tetrahedron Letters 43(8) (2002): 1473-1475.

[38] Awale, S., Tezuka, Y., Banskota, A.H., Shimoji, S., Taira, K., and Kadota, S. Norstaminane- and isopimarane-type diterpenes of *Orthosiphon stamineus* from Okinawa. Tetrahedron 58(27) (2002): 5503-5512.

[39] Di, X.-X., Wang, S.-Q., Zhang, X.-L., Wang, B., Lou, H.-X., and Wang, X.-N. Diterpenoids from the aerial parts of *Orthosiphon aristatus* var. *aristatus*. Phytochemistry Letters 6(3) (2013): 412-417.

[40] Ohashi, K., Bohgaki, T., Matsubara, T., and Shibuya, H. Indonesian medicinal plants. XXIII. Chemical structures of two new migrated pimarane-type diterpenes, neoorthosiphols A and B, and suppressive effects on rat thoracic

aorta of chemical constituents isolated from the leaves of *Orthosiphon aristatus* (Lamiaceae). Chemical & Pharmaceutical Bulletin 48(3) (2000): 433-435.

[41] Mi, K.P., Yong, Y.L., and Hye, S.Y.C. Anti-platelet effect of the constituents isolated from the barks and fruits of *Magnolia obovata.* Archives of Pharmacal Research 25(3) (2002): 325-328.

[42] Syafni, N., Putra, D.P., and Arbain, D. 3,4-dihydroxybenzoic acid and 3,4-dihydroxybenzaldehyde from the fern Trichomanes chinense L.; isolation, antimicrobial and antioxidant properties. Indonesian Journal of Chemistry 12(3) (2012): 273-278.

[43] Wang, Z.J., Zhao, Y.Y., Wang, B., Ai, T.M., and Chen, Y.Y. Depsides from *Prunella vulgaris.* Chinese Chemical Letters 11(11) (2000): 997-1000.

[44] Lin, L., Dong, Y., Zhao, H., Wen, L., Yang, B., and Zhao, M. Comparative evaluation of rosmarinic acid, methyl rosmarinate and pedalitin isolated from *Rabdosia serra* (MAXIM.) HARA as inhibitors of tyrosinase and α-glucosidase. Food Chemistry 129(3) (2011): 884-889.

# APPENDIX

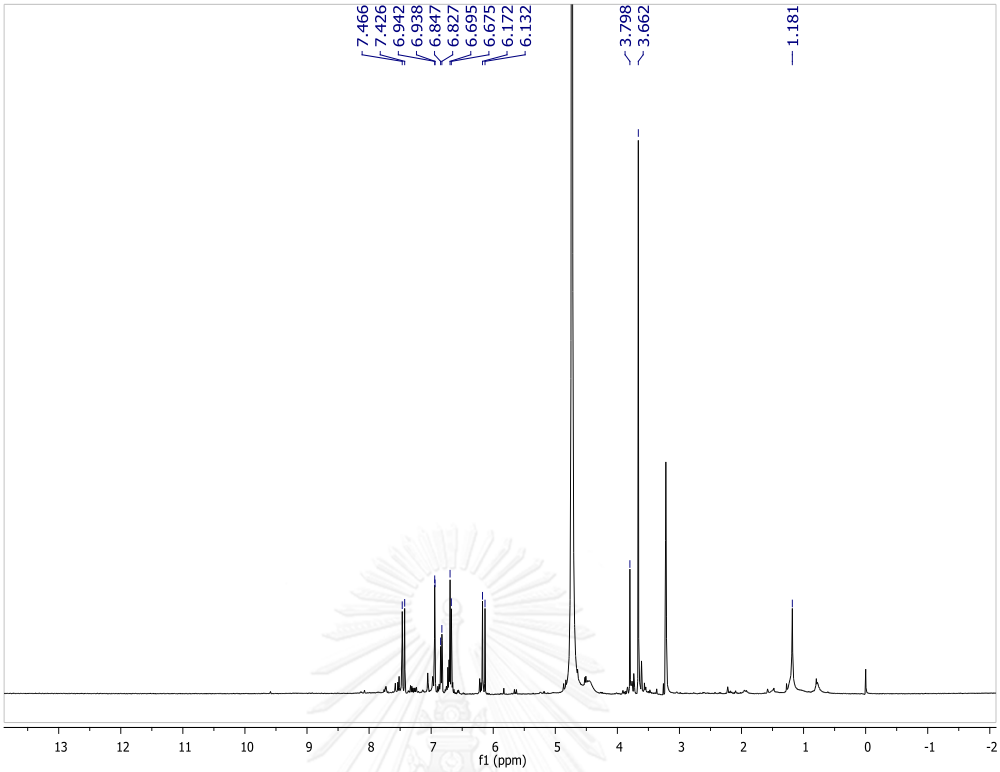


**Figure 1** $^{1}$H NMR ($CD_3OD$) spectrum of methyl caffeate (**1**)

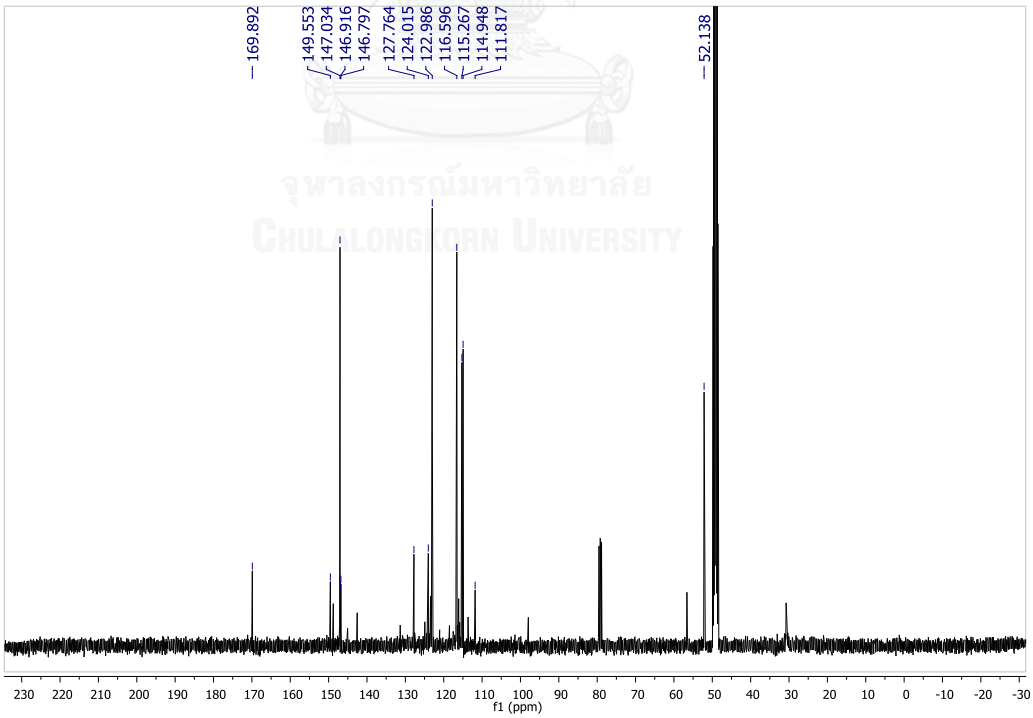


**Figure 2** $^{13}$C NMR ($CD_3OD$) spectrum of methyl caffeate (**1**)

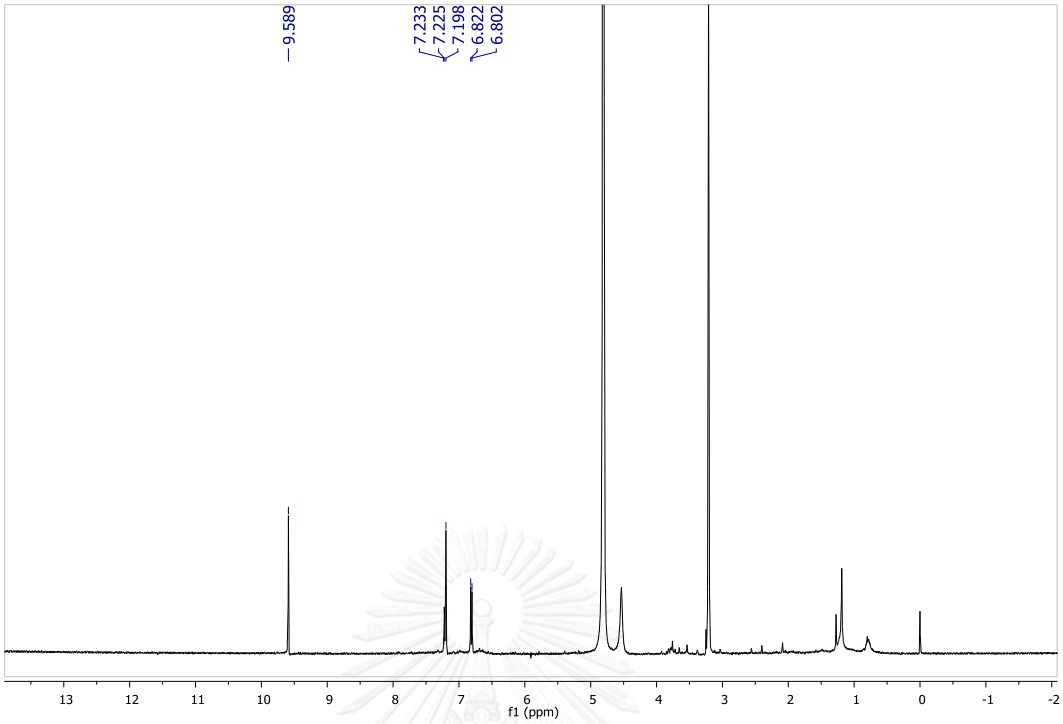


**Figure 3** $^{1}$H NMR ($CD_3OD$) spectrum of 3,4-dihydroxybenzaldehyde (**2**)

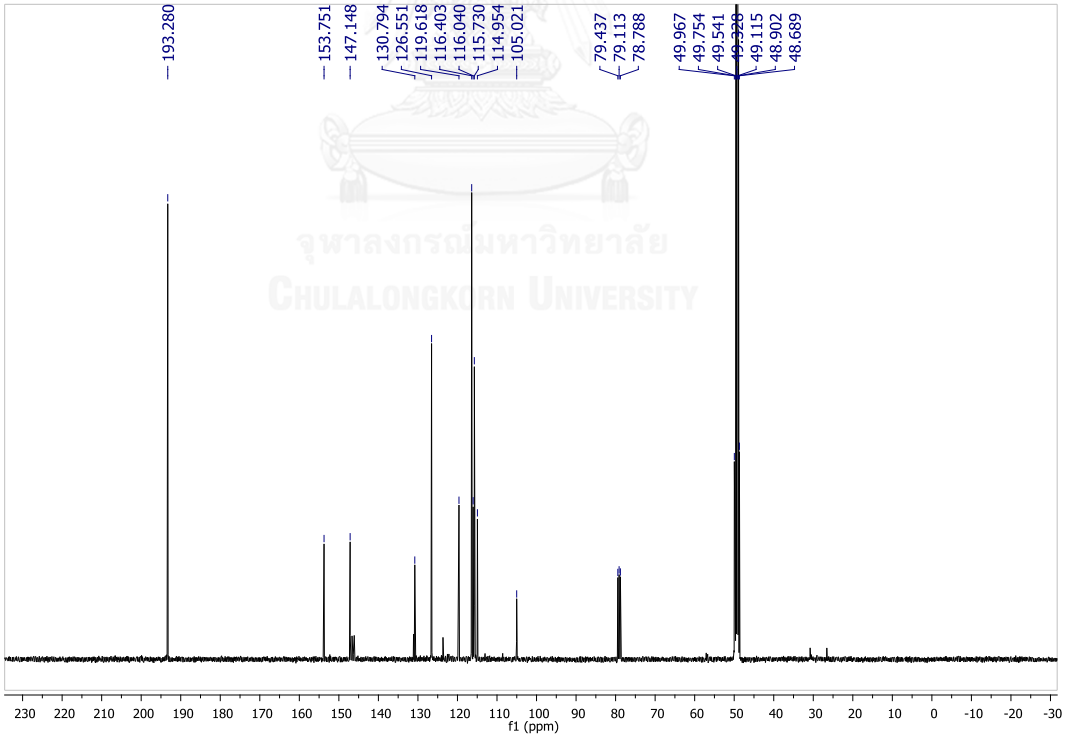


**Figure 4** $^{13}$C NMR ($CD_3OD$) spectrum of3,4-dihydroxybenzaldehyde (**2**)

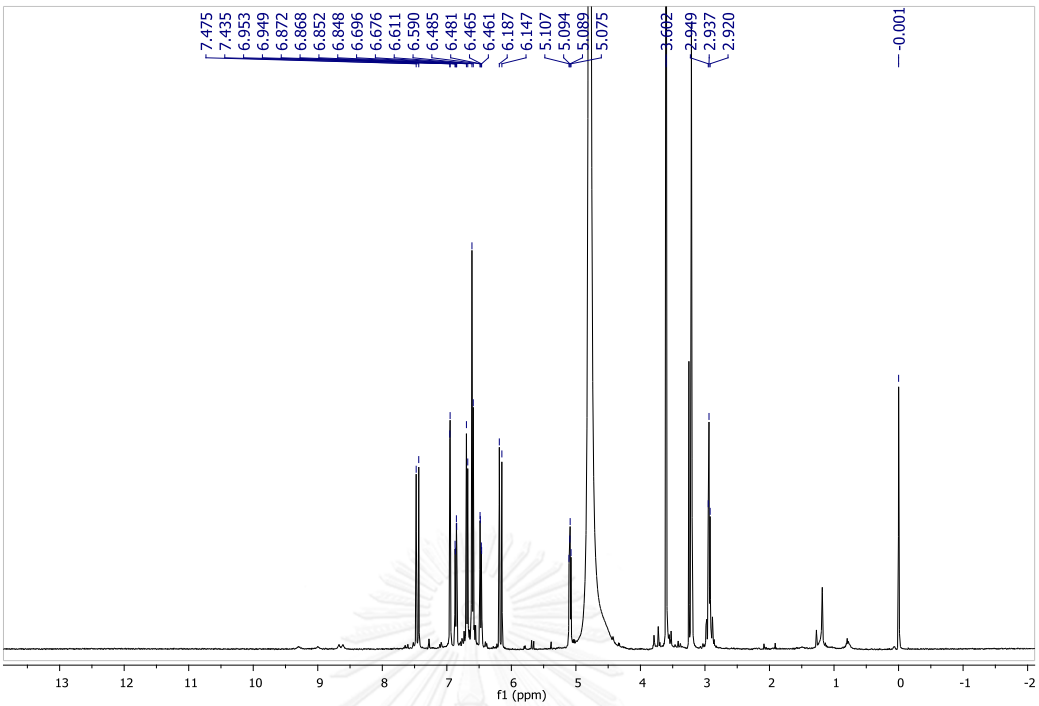


**Figure 5** $^{1}$H NMR ($CD_3OD$) spectrum of methyl rosmarinate (**3**)

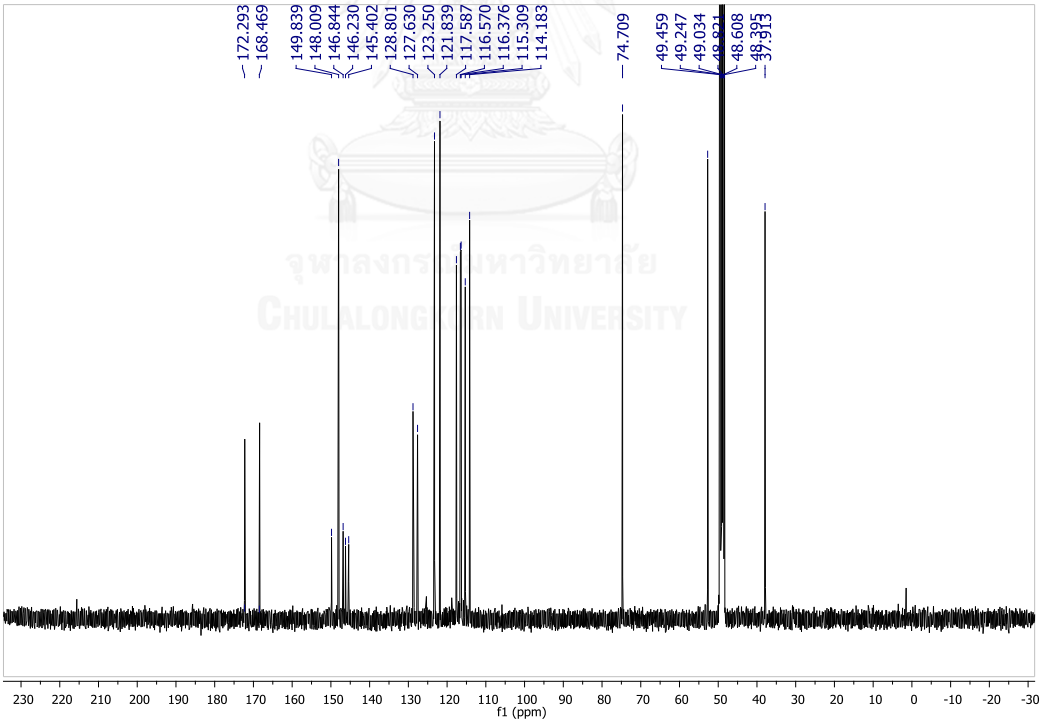


**Figure 6** $^{13}$C NMR ($CD_3OD$) spectrum of methyl rosmarinate (**3**)

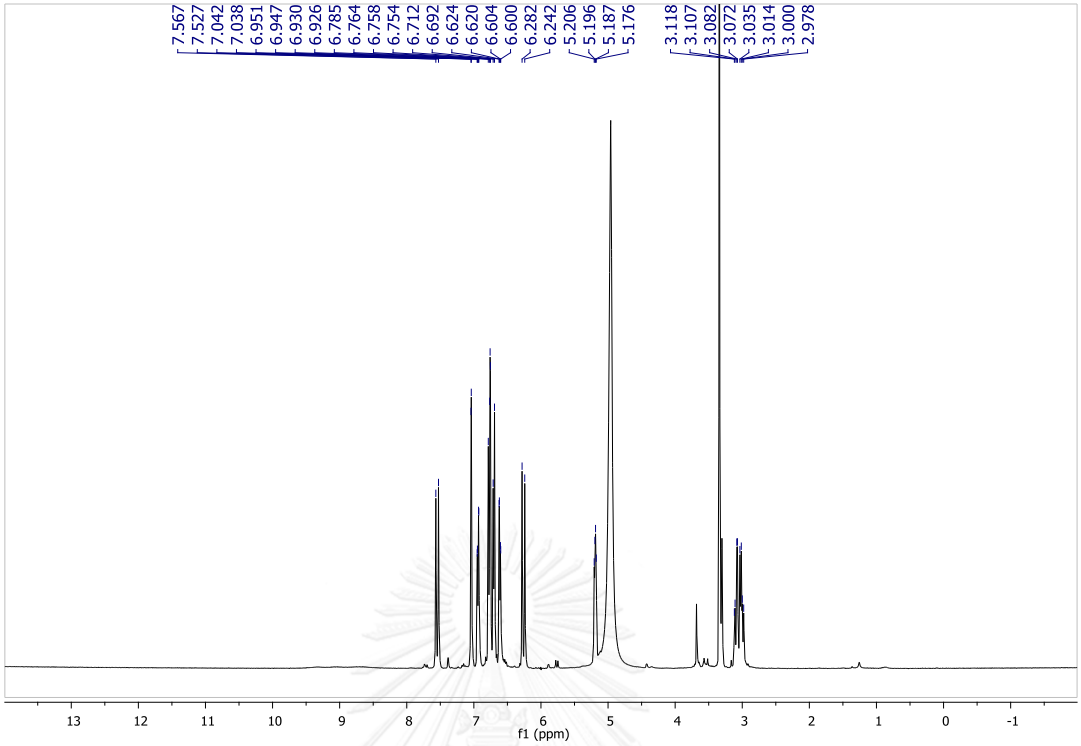


**Figure 7** $^{1}$H NMR ($CD_3OD$) spectrum of rosmarinic acid (**4**)

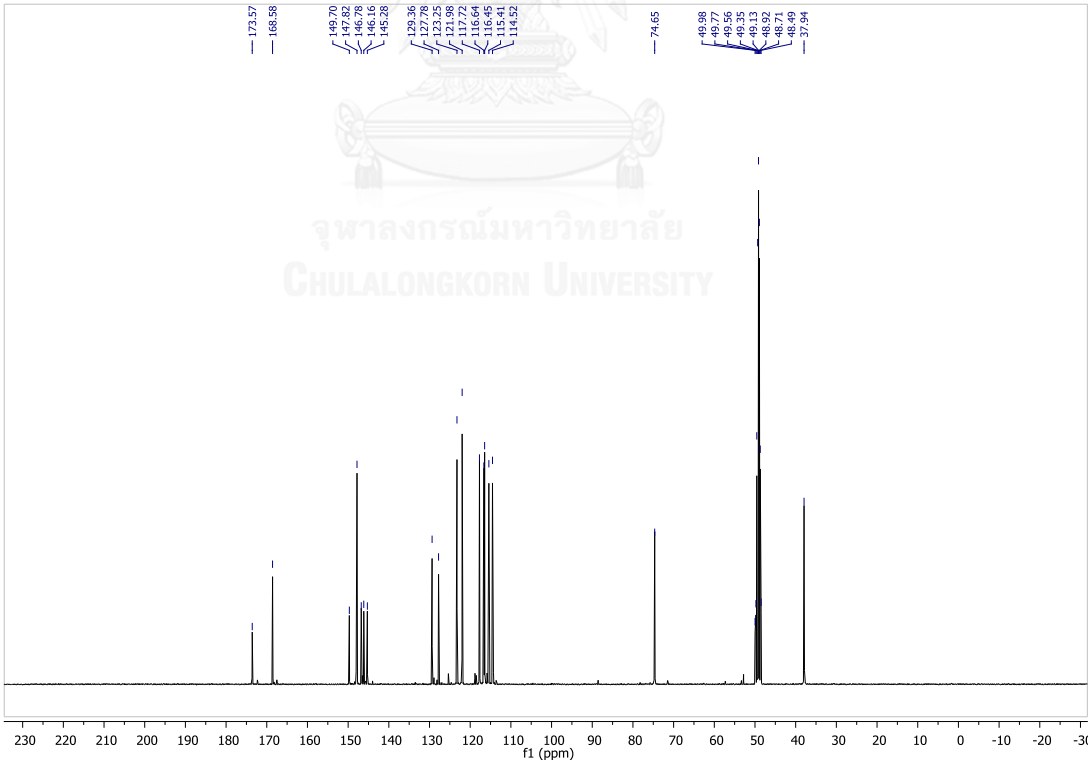


**Figure 8** $^{13}$C NMR ($CD_3OD$) spectrum of rosmarinic acid (**4**)

# VITA

Miss Doungkamon Toumsuk was born on May19, 1986 in Bangkok, Thailand. She graduated with Bachelor' s Degree of Science in Biotechnology from Faculty of Science, King Mongkut's Institute of Technology Ladkrabang, in 2008.During studying in Master Degree inBiotechnology program, she attended conference proceedings of International Bioscience Conference (IBSC 2014) in the topic of **α**-GLUCOSIDASE INHIBITORS FROM JAVA TEA Orthosiphon aristatus (Blume) Miq.